Supporting Information

Microchip emitter for solid phase extraction-gradient elution-mass

spectrometry

Natalia Gasilova, Liang Qiao, Dmitry Momotenko, Mohammad Reza Pourhaghighi and Hubert

H. Girault*

Laboratoire d'Electrochimie Physique et Analytique, Ecole Polytechnique Fédérale de Lausanne,

Station 6, CH-1015 Lausanne, Switzerland

*Hubert H. Girault, e-mail: hubert.girault@epfl.ch; phone: +41 (0)21 693 31 51; fax: +41 (0)21

693 36 67

SI-1: Chemicals and Materials

Reverse phase chromatography (RPC) C_{18} and C_8 coated superparamagnetic beads (1.08 µm diameter) were purchased from Invitrogen (Oslo, Norway) and Bioclone Inc. (San Diego, CA, USA), respectively. Insulin chain B (from bovine pancreas), bradykinin (acetate salt, ≥98%), peptide MRFA (acetate salt, ≥90%) were obtained from Sigma-Aldrich (Buchs, Switzerland). All other peptides were purchased from Bachem (Dübendorf, Switzerland). Trypsin (from bovine pancreas) was obtained from Applichem (Darmstadt, Germany). Myoglobin (horse heart, 90%), 2,5-dihydroxybenzoic acid (98%) were obtained from Sigma-Aldrich (Buchs, Switzerland). Acetic acid (99.5%), trifluoroacetic acid (TFA), ammonium bicarbonate (99.5%) were purchased from Fluka (Buchs, Switzerland). Methanol (>99%) was obtained from Merck (Darmstadt, Germany) and acetonitrile (99.9 %) from ABCR (Karlsruhe, Germany). Human plasma was purchased from Bioreclamation LLC (Westbury, NY, USA). For sample solutions and all experiments, deionized water produced by an alpha Q-Millipore System (Zug, Switzerland) was used. To retain the magnetic beads inside the microchip chamber four permanent cylindrical magnets (Nd-Fe-B, 1 mm diameter, 1 mm length, Supermagnete, Zürich, Switzerland) were used.

Fused silica capillaries (75 µm i.d, 30 cm length, BGB analytik AG, Böckten, Switzerland) formed the connections between glass syringes (Hamilton, Bonaduz, Switzerland) in the syringe pumps (Cole Palmer Instrument Company, Vernon Hills, USA) and a homemade plastic microchip holder with tight fittings (IDEX Health and Science LLC, Oak Harbor, WA, USA) to perform solution injections into the microchip.

SI-2: Microchip fabrication

An solid phase extraction-gradient elution-mass spectrometry (SPE-GEMS) microchip was fabricated using a scanning laser ablation method. All microchannels were drilled in a polyimide (PI) substrate (125 μm thick, DuPont™Kapton® polyimide film, Dupont, Geneva, Switzerland) by photoablation with an ArgonFluoride excimer laser (Lambda Physics LPX 210I, Göttingen, Germany). The laser was operated at 193 nm with pulse width about 20 ns, fluence = 0.35 J and frequency = 50 Hz. The depth and width of all microchannels are 50 µm and 100 µm, respectively. A round chamber (500 µm diameter, 50 µm depth) for trapping of magnetic beads was created using laser ablation in a static shot mode. The quality of photoablated substrate was inspected under a laser scanning microscope VK-8710 (Keyence Corporation, Osaka, Japan). The electrode microchannel was filled with conductive carbon ink (Electrador, Electra Polymer & Chemicals Ltd., UK) and the substrate was cured for 30 min at 80ºC in the oven. Finally, the microchip was covered with a 25/10 μm thick polyethylene/polyethyleneterephthalate (PE/PET) layer using lamination apparatus (Morane Senator, Oxon, UK) at 130ºC and 3 bars. For the lamination improvement, microchip was additionally cured for 1h at 80 °C in the oven. To facilitate the electrospray formation the tip of the microchannel A was cut in a V-shape. For the electrospray performance the microchip emitter was placed in front of the source inlet of Thermo LTQ Velos instrument (Thermo Scientific, San Jose, USA) as shown in Figure SI-2:

Figure SI-2. SPE-GEMS microchip is placed in front of the ESI-MS source inlet.

SI-3. Protein digestion and OFFGEL separation

A mixture of peptides to be analysed by SPE-GEMS was generated by the tryptic digest of myoglobin. The 5 mg/ml solution of myoglobin was first denatured by heating at 100°C for 5 min and then was incubated with 0.17 mg/ml of trypsin in a 25 mM NH_4HCO_3 buffer under 37 °C for 18 h. The reaction was stopped by freezing the digest solution for storage at -20°C. For SPE-GEMS experiment myoglobin digest was dissolved 500 times with 0.1% TFA solution to the final concentration of 560 nM and was analysed on C_8-coated Mbs.

OFFGEL separation of myoglobin digest was performed with Agilent 3100 OFFGEL fractionator (Agilent, Waldbronn, Germany) using an 18 cm immobilized pH gradient (IPG) strip pH 3-10 (Amersham Biosciences, Otelfingen, Switzerland). Prior to the separation the IPG strip was swollen with 0.1% IPG buffer (pH 3-10) solution and 50 µL of myoglobin digest (5 mg/ml) were diluted 55 times with 0.1% IPG buffer (pH 3-10). Each of 18 fractionation wells was loaded with 150 µL of sample and the focusing was carried out during 14 h with the current and voltage limited to 100 µA and 6 kV respectively. Additional 4 h of focusing were performed with the current and voltage limited to 150 µA and 8 kV respectively. 18 fractions collected after OFFGEL separation were analysed by MALDI-MS in order to verify the quality of separation. The solutions collected from 8th and 14th wells (pH 5.9 and 8.4 respectively) were also studied by ESI-MS mass spectrometer with commercial ionization source and then were diluted 50 times and submitted to SPE-GEMS analysis diluted on C_8-coated Mbs.

SI-4. Optimization of the microchip desing and parameters of SPE-GEMS experiment

SPE-GEMS microchip was designed in order to perform effective sample preconcentration on Mbs as SPE sorbent and gradient elution with simultaneous ESI-MS detection. The chamber for Mbs trapping was introduced in order to increase the amount of Mbs that could be loaded inside the microchip. Different chamber E diameters (d= 400÷700 µm) for Mbs trapping by permanent magnets were assessed during chip configuration development. The stability of Mbs packaging in the chambers of different size was checked by observation of Mbs behavior under the application of a water-methanol mixture (1:1) at a flow rate of 40 µL/h. The observations were made under a laser microscope with one magnet (top one) removed. The best Mbs stability and distribution allowing proper contact of the liquid flow with the SPE sorbent were achieved in the chamber with 500 µm of diameter. Smaller chamber was easily blocked by loaded Mbs. In larger chambers there was no permanent contact of the flow with the Mbs: the chambers were non-uniformly filled with the liquid and were accumulating the air bubbles occasionally introduced inside the microfluidic system.

For creation of a step-wise gradient of organic solvent inside the main channel A, this channel was jointed with two microchannels B and C introduced for injection of water and methanol, respectively. An optimal distance between the junctions of channels B and C with channel A and the chamber E was set at 1.4 cm in order to ensure the proper mixing of water and methanol solutions injected *via* channel B and C, respectively. This value was chosen according to performed numerical finite element simulations showing that the good mixing of water with the methanol is achieved after 1.35 cm from channels junction (data not shown).

In order to decrease the broadening of peptide bands eluted from Mbs due to diffusion/convection processes within laminar flow established in a microchannel the distance between the chamber E and the emitting tip of the microchip should be minimal. Based on this assumption the junc-

tions of channel D and electrode with channel A as well as the distance between the electrode and microchip tip were chosen with smallest possible values which still enable the correct operation of the microfluidic system.

The amount of SPE sorbent (25 µg of Mbs) was adjusted to provide enough efficiency for preconcentration of the diluted samples (see below) without blocking the channels and chamber with Mbs and ensuring the proper flushing of the microchip between the experiments. The chosen total flow rate during gradient elution of trapped peptides was, on the one hand, enough to give a stable electrospray from the microchip tip even without a sheathflow. On the other hand, this flow rate was not leading to the loss of Mbs from the chamber.

The sheathflow channel D was introduced into the microchip to provide a stable electrospray and ion current during the SPE-GEMS experiments. Electrospray quality strongly depends on the organic solvent amount in the liquid to spray: methanol presence decreases the surface tension of the spraying droplet facilitating its vaporization and ions formation (Batista da Silva, J. A.; Brady Moreira, F. G.; Leite dos Santos, V. M.; Longo, R. L. *Phys. Chem. Chem. Phys.*, **2011**, *13*, 6452–6461). The ESI buffer containing 50% of methanol was injected *via* a channel D always keeping sufficient percentage of organic solvent in spraying solution. It is especially crucial at the beginning of gradient elution process when the eluent contains only 5% of methanol. However, the sheathflow dilutes the peptide fractions eluted from Mbs. In order to minimize this effect the flow rate of ESI buffer in channel D was set to 10 µL/h.

The gradient timing was adjusted to provide sufficient stability for ESI ion current during analysis. The changes of microfluidic rates could destabilize the electrospray therefore the raise of methanol amount in eluent solution every 3.5 min was chosen as an optimal gradient timing that allowed stable spray maintaining with good sensitivity of the analysis and reasonable experimental time.

Prior to SPE-GEMS experiments with model peptide mixtures developed microfluidic system was tested for nonspecific adsorption of samples inside the microchip channels. The injection of peptide mixture 1 (14 µL of 10 µM solution) to the microchip was performed followed by washing with 10 µL

of water. Then 50% methanol solution was injected and electrospray was initialized for ESI-MS detection of eluted peptides. The same experiment was performed with peptide mixture 2 (10 µM). No peptides of interest were observed on obtained ESI-MS spectra in both cases (data not shown) confirming the absence of strong nonspecific sample adsorption inside the microchip channels.

SI-5: SPE-GEMS analysis of model peptide mixtures at concentration of 1μM and its separation characteristics

Herein, the results obtained during the SPE-GEMS analysis of model peptide mixtures at concentration of 1 µM are presented in Figures SI-5.1 and SI-5.2.
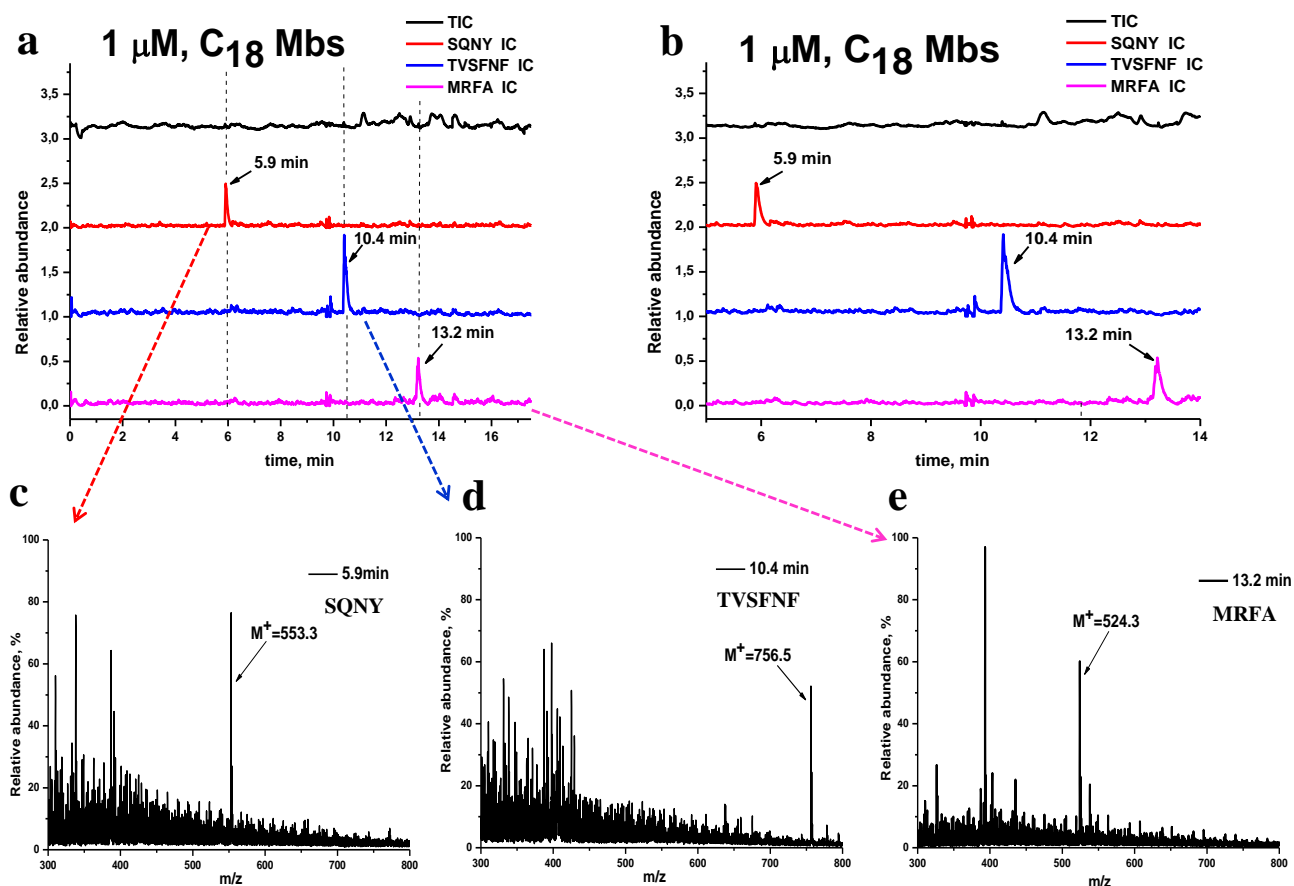

Figure SI-5.1. SPE-GEMS analysis of peptide mixture 1 on C_{18}-coated Mbs. a) IC chromatograms of peptide ions and total IC during elution. b) Zoomed view of the IC chromatograms of peptide ions. c), d), e) ESI-MS spectra obtained during elution of peptides of mixture 1. For the analysis 10 µL of 1 µM sample solution was loaded into the microchip. The timescale for the stepwise gradient elution was the following: 0 min – 5% of methanol in eluent mixture, 3.5 min – 10%, 7 min – 20%, 10.5 min – 30%, 14 min – 40%.

Figure SI-5.2. SPE-GEMS analysis of peptide mixture 2 on C_8-coated Mbs. a) IC chromatograms of peptide ions and total IC during elution. b) Zoomed view of the IC chromatograms of peptide ions. c), d), e) ESI-MS spectra obtained during elution of peptides of mixture 2. For the analysis 10 µL of 1 µM sample solution was loaded into the microchip. The timescale for the stepwise gradient elution was the following: 0 min – 5% of methanol in eluent mixture, 3.5 min – 10%, 7 min – 20%, 10.5 min – 30%, 14 min – 40%.
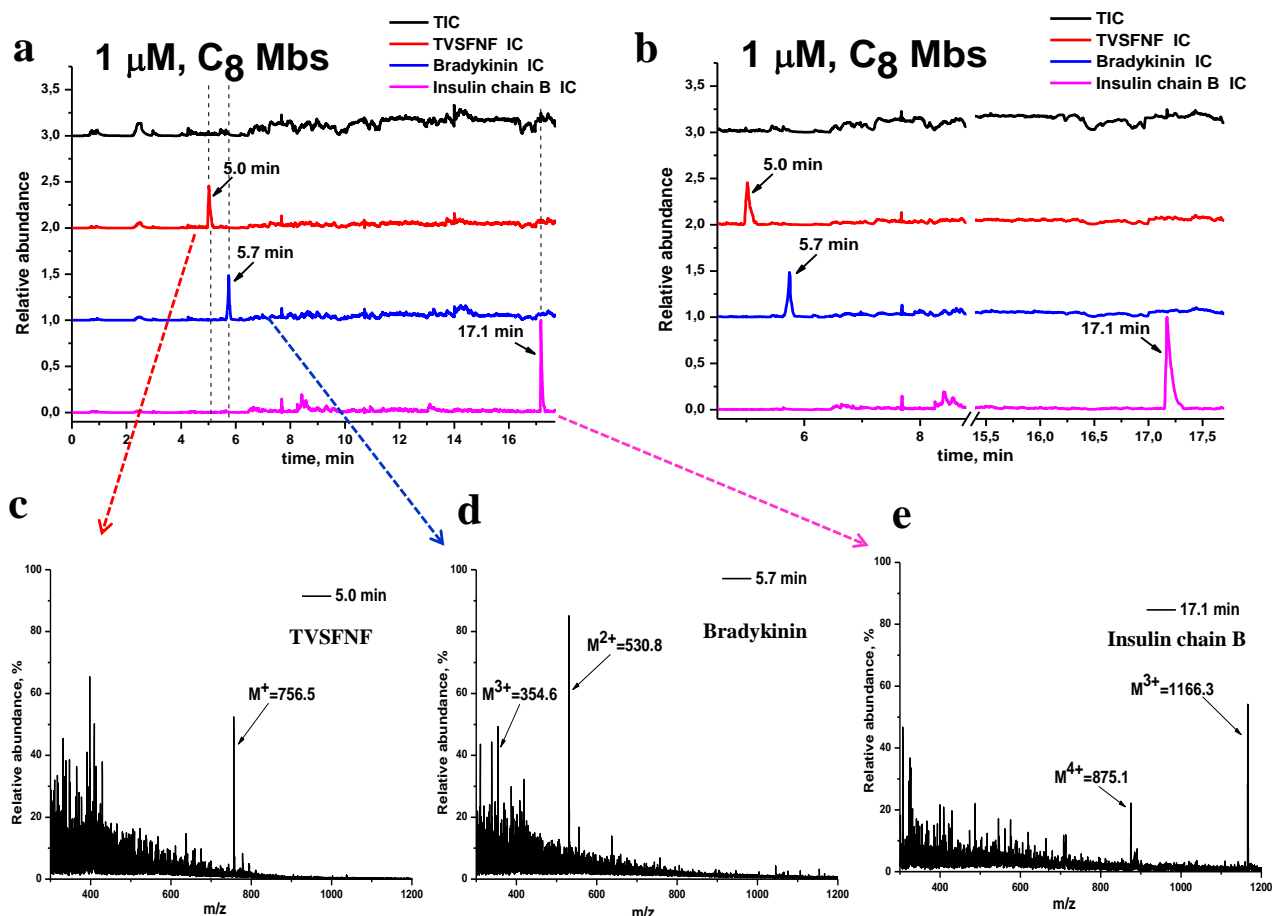
Effect of saturation of SPE support. During the SPE-GEMS analysis of model mixtures with 10 nM, 25 nM and 100 nM peptide concentrations there was a linear correlation between the initial amount of peptides in a sample and signals obtained, while for 1 µM solution the signal saturation was encountered due to SPE support saturation. For example, in case of TVSFNF peptide analysis on C_{18}-Mbs the average signal-to-noise ratio S/N observed on IC chromatograms for 10 nM solution was 3.5, for 25 nM was 6, for 100 nM was 17 and only 24 for 1 µM peptide mixtures (see Figure SI-5.1). Such behavior is in good correlation with the Mbs binding capacity presented by the manufacturer if the points presented below are taken into account. The published binding capacity is normally presented only for

one particular peptide and varies significantly from one peptide to another (http://tools.invitrogen.com/content/sfs/manuals/102%2011D12D%20Dynabeads%20WCX%20%28rev002%29.pdf). In case of C_{18}-Mbs the binding capacity is presented as approx. 14 μg (10 nmol) of the peptide SGAIEGRGSGSGSC (MW 1,380, 14 amino acids) for 1 mg of Mbs, *i.e.* 250 fmol of peptide for 25 μg of Mbs loaded inside of SPE-GEMS microchip. As TVSFNF peptide consists only of 7 amino acids and has more hydrophobic residues it is possible to assume that for this peptide the maximal binding capacity will be at least two times higher, 500 fmol of peptide per 25 μg of Mbs. Meanwhile, during the experiment with 10 nM peptide mixture solution 100 fmol of peptide are injected, for 25 nM solution 250 fmol of peptide are injected, for 100 nM – 1 pmol of peptide and for 1μM solution – 10 pmol. In theory the saturation should be reached already in case of 100 nM peptide solution which is not observed experimentally as in practice not all injected sample is adsorbed on the Mbs. However, when the 1 μM peptide solution is analysed the sample is presented in such an excess that the clear Mbs saturation is encountered. So developed SPE-GEMS technique is more suitable for analysis of diluted samples which do not provoke the saturation of SPE support used. It is also worth to mention that for C_8-Mbs the published binding capacity is presented as 20 μg of protein/peptide per 1 mg of Mbs (http://www.bioclone.us/files/BcMag_C-4-C-8_Magnetic_Beads.pdf) which for the peptide TVSFNF could be recalculated as ∼ 715 fmol of peptide per 25 μg of Mbs.

Characterization of SPE-GEMS analysis as a separation technique. The SPE-GEMS experiments performed with model peptide mixtures 1 and 2 shown the possibility not only to preconcentrate but also to separate the components of chosen samples. For description of SPE-GEMS analysis as a separation technique the peak efficiency of the system was provided: the average resolutions of separation were calculated based on the results displayed below in Table SI-5 for model peptide mixtures 1 and 2 as 21 and 22 respectively.

Table SI-5. Separation characteristics obtained for SPE-GEMS analysis of model peptide mixtures.

Peptide	C_{18}-coated Mbs			C_8-coated Mbs		
	SQNY	*TVSFNF*	*MRFA*	*TVSFNF*	*Bradykinin*	*Insulin chain B*
t_R, min	5.6 ± 0.6	11 ± 1	13.5 ± 0.7	4.6 ± 0.5	5.2 ± 0.7	16.4 ± 1
Δw, min	0.20 ± 0.03	0.36 ± 0.04	0.46 ± 0.05	0.16 ± 0.03	0.18 ± 0.02	0.19 ± 0.03

t_R – average retention time (*n*=3), Δw - average width (n=3) of the elution profile peaks of peptides on IC chromatograms obtained for model peptide mixtures at 1μM concentration.

Indeed, obtained values characterize only the separation of these particular peptide mixtures which contain only 3 components easily separable from each other. As a SPE based technique the SPE-GEMS analysis possesses in general limited peak capacity. One of the key factors for successful resolving of all mixture components is the range of the extraction constant $K_{extraction}$ values of the components. According to the results presented in mathematical modeling part of the current manuscript, for two components to be resolved for 80 % during elution after SPE the values of their $K_{extraction}$ should differ for 100 times. That means that the peak capacity of the SPE-GEMS system strongly depends on the sample nature. For complex samples, *e.g.* myoglobin digest, the peak efficiency is low and it is difficult to significantly improve the peak capacity due to large amount of sample components possessing close $K_{extraction}$ values. In this case the success of developed analysis for such complex sample relies on the re-solving power of the MS detection. This is an advantage of SPE-GEMS system which allows ignoring the necessity of peak capacity improvement from chromatographic point of view to certain extends. If such improvement is still required an optimization of several experimental parameters is possible. The step-gradient elution currently used for SPE-GEMS experiment should be replaced by linear gradient of organic solvent. The fraction broadening during diffusion should be decreased by modification of micro-chip design: the distance that sample flows after elution from Mbs chamber to the tip should be minimize as much as possible. Also the optimization of volumic flow rate $F_v \cdot V_m^{-1}$ values as it is demonstrated in the mathematic modeling part of the manuscript could increase the peak capacity of the system because this parameter influences significantly the sample elution profile.

SI-6: Comparison of SPE-GEMS technique with plain microhip emitter

For comparison of SPE-GEMS technique with the plain microchip emitter, the model peptides in pure ESI buffer (50% of methanol, 49% of water and 1% of acetic acid) and model peptides in ESI buffer containing 1 mM of NaCl were sprayed to ESI-MS instrument *via* SPE-GEMS microfluidic device without Mbs in the preconcentration chamber. In order to avoid the presence of mutual ion suppression effect every component of the model mixtures was injected and analysed separately. During these experiments the same conditions as the ones implemented in typical SPE-GEMS analysis including the presence of sheathflow were used.

As was expected the detection sensitivity provided by the microchip emitter was found to be higher than the one of the commercial ionization source if the sample flow rate and spraying voltage are used. LODs for model peptide mixtures in ESI buffer were defined as 150 nM for all peptides. Enrichment factor values provided by SPE-GEMS analysis in relation to the plain microchip emitter system are presented below in Table SI-6:

Table SI-6. Enrichment factors (EF) obtained for SPE-GEMS analysis of model peptide mixtures.

		C_{18}-coated Mbs			C_8-coated Mbs		
Spraying system to compare	*Peptide*	*SQNY*	*TVSFNF*	*MRFA*	*TVSFNF*	*Bradykinin*	*Insulin chain B*
	t_R, **min**	5.6 ± 0.6	11 ± 1	13.5 ± 0.7	4.6 ± 0.5	5.2 ± 0.7	16.4 ± 1
Commercial source	$EF_{vs\ ESI\ buffer}$	12	23	13	10	10	20
	$EF_{vs\ 1mM\ NaCl}$	500	1065	530	470	400	1200
Microchip emitter	$EF_{vs\ ESI\ buffer}$	7	14	8	7	6	12
	$EF_{vs\ 1mM\ NaCl}$	120	260	130	115	100	310

t_R – average retention time (*n*=3), $EF_{vs\ ESI\ buffer}$ – EF of SPE-GEMS (25 nM) in comparison with a classical ESI-MS detection *via* an appropriate spraying system of a single peptide (150 nM) in the ESI buffer, $EF_{vs\ 1mM\ NaCl}$ – EF of SPE-GEMS (25 nM) in comparison with a classical ESI-MS detection *via* an appropriate spraying system of a peptide solution (2.5 µM) containing 1 mM NaCl in the ESI buffer.

The difference between EF values obtained for SPE-GEMS analysis in relation to commercial ionization source and to microchip emitter allows estimating the importance of the spraying source nature. Since the spaying and ionization conditions are the same for plain microchip emitter and SPE-GEMS microfluidic device appropriate EFs represent only the contribution of sample preconcentration and purification on Mbs. For example for peptide TVSFNF on C_{18}-Mbs such EF is 14. When the comparison is made with commercial ionization source, *i.e.* the spraying source nature also contributes to

improvement of sensitivity, the EF for peptide TVSFNF increases for ~1.67 times giving the value of 23. Therefore the type of spraying and ionization source is significant for the sensitivity of the analysis.

Similar tendencies were observed for analysis of samples containing 1 mM of salt. Microchip emitter was more tolerant to the salt presence in the sample providing the LODs for all peptides of 2.5 µM in contrast with 10 µM of LODs for commercial ionization source. EFs calculated for salt containing samples are also presented in Table SI-6. In this case the contribution of spraying source nature in SPE-GEMS analysis increases the sensitivity of sample detection for ~4 times providing, for example for peptide TVSFNF on C_{18}-Mbs, EF of 1065 in relation with commercial ionization source. However, the desalting efficiency of SPE-GEMS technique estimated independently from type of spraying system is also high: the EF values in relation to the microchip emitter are in the range of 100-310. Sample desalting and purification step remains a crucial point during SPE-GEMS analysis.

SI-7: MALDI and ESI-MS analysis of model peptide mixtures using commercial protocol of SPE on Mbs
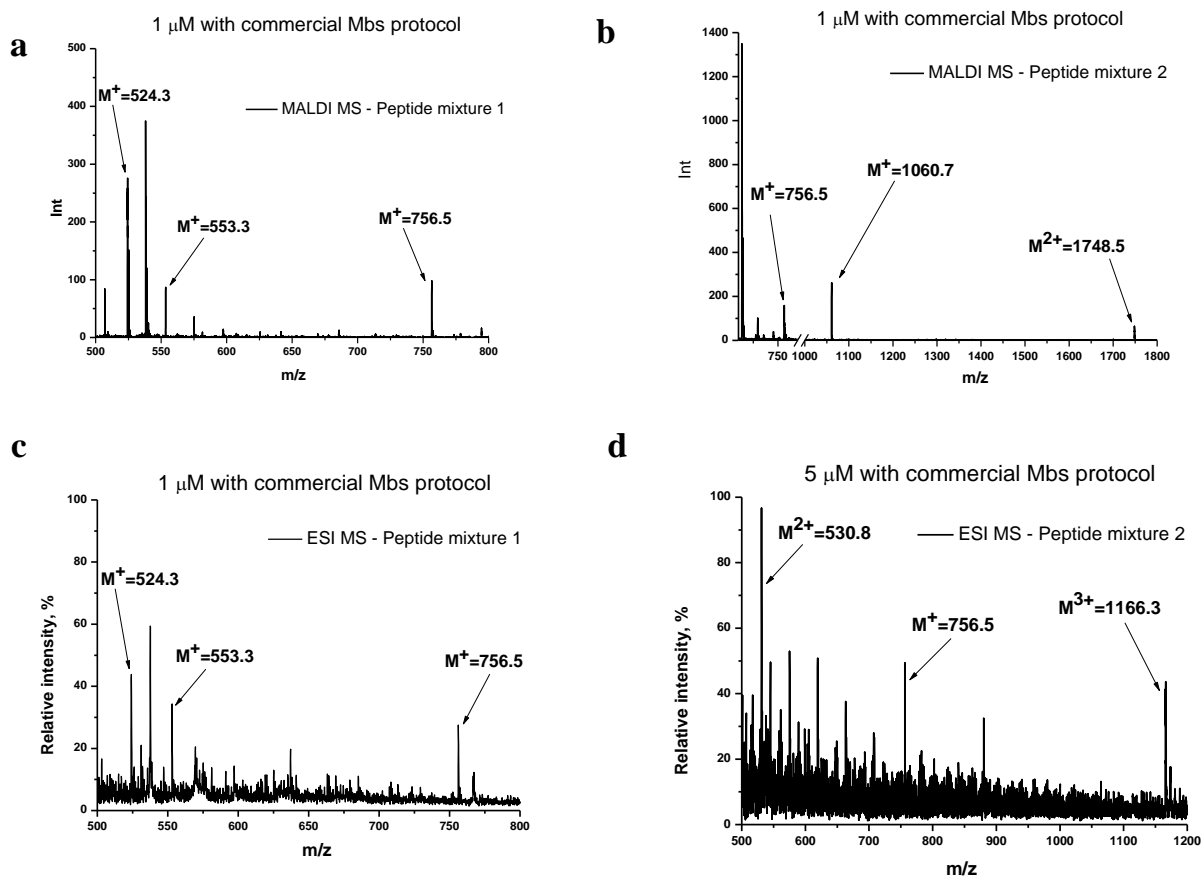

Figure SI-7. MS spectra of peptide model mixtures processed according to the commercial protocol of SPE on Mbs. a), b) MALDI-MS spectra of 1 µM peptide model mixtures 1 and 2, respectively. c), d) ESI-MS spectra of peptide model mixtures 1 (1 µM) and 2 (5 µM), respectively. For commercial protocol of SPE on Mbs 250 µg of C_{18} Mbs or 500 µg of C_8 Mbs were incubated with 100 µl of appropriate peptide mixture. 0.1% TFA. 25 µl of 50% acetonitrile solution was used as elution buffer. For MALDI-MS matrix solution was composed of 10 mg/mL solution of 2,5-dihydroxybenzoic acid in 50% water and 50% acetonitrile. Ions marked on the plots correspond to the following peptides: 524.3= M^+(MRFA), 553.3= M^+(SQNY), 756.5= M^+(TVSFNF), 530.8= M^{2+} and 1060.7= M^+ (bradykinin), 1748.5= M^+ and 1166.3= M^{3+}(insulin chain B). Experiments were repeated in triplicates.

Due to the high salt concentration in washing and sample solutions (200 mM and 800 mM NaCl, respectively) used in SPE on C_8-coated Mbs following the commercial protocol the ESI-MS spectra for

the peptide mixture 2 were obtained with high level of noise and with LOD of 5μM, while MALDI-MS

detection gave good results already for 1μM solution of peptide mixture 2 processed on these Mbs.

SI-8: Analytical model of sample elution process

To account for the elution process it is necessary to consider partition equilibrium of analyte between the mobile (solution) and the stationary (Mbs) phases as shown in Figure SI-8.1:

$$a_{mobile} \leftrightarrow a_{stationary}$$
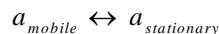
where $a_{stationary}$ and a_{mobile} denote the analyte species in the respective phases.

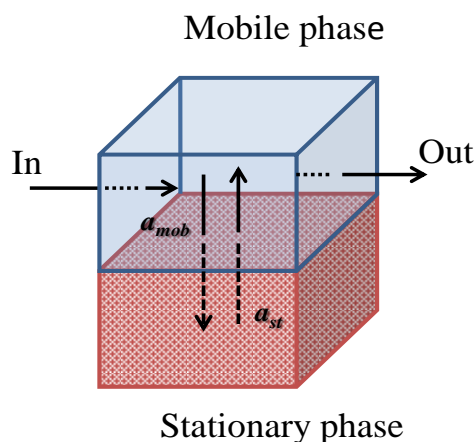Mobile phase

Stationary phase

Figure SI-8.1. Schematic representation of analyte a partition between mobile and stationary phases.

The partition constant K_p can be expressed by the capacity factor k' and the volume phase ratio $\left(\phi = V_s / V_m \right)$

$$K_p = \frac{k'}{\phi} = \frac{1-p}{\phi p} \tag{1}$$

where p is the probability of partition in the mobile phase. Assuming equilibrium between the two phases, it is possible to write

$$\Delta G_p^0 - RT \ln K_p = 0 \tag{2}$$

where R and T specify gas constant and temperature, and ΔG^0_p is the standard Gibbs energy of partition. The mobile phase is a binary solvent mixture that could be described by parameter α denoting the molar fraction of organic solvent in a water/organic solvent bicomponent mixture. The standard Gibbs energy

of solvation in the mobile phase, ΔG^0_{mobile} , can be assumed to be a linear combination of the Gibbs energies of hydration and solvation in the pure organic solvent (marked with corresponding indexes w and o)

$$\Delta G^0_{mobile} = (1 - \alpha)\Delta G^0_w + \alpha \Delta G^0_o = \Delta G^0_w + \alpha (\Delta G^0_o - \Delta G^0_w) = \Delta G^0_w + \alpha \delta \quad . \tag{3}$$

where δ denotes the difference of solvation energies between the pure organic solvent and water. As the partition energy is defined as the difference in the solvation energy between the stationary and the mobile phases, equation 2 could be rewritten:

$$\Delta G^0_p = (\Delta G^0_{stationary} - \Delta G^0_{mobile}) = (\Delta G^0_{stationary} - \Delta G^0_w) - \alpha \delta \tag{4}$$

where $(\Delta G^0_{stationary} - \Delta G^0_w)$ represents the standard Gibbs energy of extraction of the analyte from the original aqueous solution, i.e. the sample, which can also be defined as a function of the extraction constant $K_{extraction}$. Finally, taking into account a linear solution composition change rate $\beta = \alpha \cdot t^{-1}$ the variation of Gibbs energy of partition with time t is obtained

$$\Delta G^0_p = -RT \ln K_{extraction} - \beta \delta t \quad . \tag{5}$$

Combination of equations 1−5 gives the expressions for K_p and p

$$K_p = \exp\left(-\frac{\Delta G^0_p}{RT}\right) = K_{extraction} \exp\left(\frac{\beta \delta}{RT}t\right) \quad ,$$

$$p = \frac{1}{1 + \phi K_{extraction} \exp\left(\dfrac{\beta \delta}{RT}t\right)} \tag{6}$$

Considering the volume element dV_m the variation of solute mass in the complete cell J as a function of time is given by

$$dm(J,t) = dm(J,t)\big|_{in} - dm(J,t)\big|_{out} = Mc_m(J-1,t)dV_m - Mc_m(J,t)dV_m =$$

$$= \left[\frac{pm(J-1,t)}{V_m} - \frac{pm(J,t)}{V_m}\right]dV_m$$

17

where M and c_m denoting molar mass and concentration of solute species in mobile phase. The resulting differential equation for analyte is

$$\frac{dm(J,t)}{dt} + p\frac{F_v}{V_m}\left[m(J,t) - m(J-1,t)\right] = 0 \tag{7}$$

where F_v is the volumic flow rate of mobile phase.

If the system is considered as a series of N cells, the system of differential equations should be solved as in the Martin and Synge model. Here, if only the first cell (J=1) is considered, there is a homogeneous equation

$$\frac{dm(t)}{dt} + p\frac{F_v}{V_m}dt = 0 \tag{8}$$

After rearrangement, equation 8 is

$$\frac{dm(t)}{m(t)} = -\frac{F_v}{V_m}\frac{dt}{1+\phi K_{extraction}\,\exp\left(\dfrac{\beta\delta}{RT}t\right)}$$

with initial condition for initial amount of analyte in the stationary phase

$$m(t)\big|_{t=0} = m_0\,.$$

The integration from 0 to t gives the solution of equation 8, which allows calculating solute concentration in the mobile phase as

$$c_m(t) = \frac{p}{V_m M}m(t) =$$

$$\frac{1}{V_m M}\left(\frac{m_0}{1+\phi K_{extraction}\,\exp\left(\dfrac{\beta\delta}{RT}t\right)}\right)\exp\left[\frac{F_v}{V_m}\frac{RT}{\beta\delta}\left(\ln\left[\frac{1+\phi K_{extraction}\,\exp\left(\dfrac{\beta\delta}{RT}t\right)}{1+\phi K_{extraction}}\right] - \frac{\beta\delta}{RT}t\right)\right] \tag{9}$$

Herein, it is convenient to represent analyte concentration and time in dimensionless form, *i.e.*

$$\frac{c_m(t)}{c_0} = \frac{1}{1+\phi K_{extraction}\exp\left(\frac{\beta\delta}{RT}t\right)} \exp\left[\frac{F_v}{V_m}\frac{RT}{\beta\delta}\left(\ln\left[\frac{1+\phi K_{extraction}\exp\left(\frac{\beta\delta}{RT}t\right)}{1+\phi K_{extraction}}\right]-\frac{\beta\delta}{RT}t\right)\right]$$

or

$$\frac{c_m(t)}{c_0} = \frac{\left[1+\phi K_{extraction}\exp\left(\frac{\beta\delta}{RT}t\right)\right]^{\frac{F_v}{V_m}\frac{RT}{\beta\delta}-1}}{\left[1+\phi K_{extraction}\right]^{\frac{F_v}{V_m}\frac{RT}{\beta\delta}}} \exp\left[-\frac{F_v}{V_m}t\right] \tag{10}$$

and t/t_{max} where t_{max} is defined through relation $t_{max}\beta = 1$.

The normalized concentration represents the fraction of analyte in mobile phase with respect to maximal possible solute concentration and time is normalized to the certain point of elution gradient, for instance $\alpha = 1$.

From this expression one could also get the retention time, *i.e.* the peak position

$$t_R = \frac{RT}{\beta\delta}\ln\left(-\frac{F_v}{V_m}\frac{RT}{\beta\delta\phi K_{extraction}}\right) \tag{11}$$

Equations 10 and 11 are the relations describing the elution process with linear elution gradient. As discussed in the main manuscript the peak shape and intensity depend on the affinity of the analyte to the organic eluent, δ. Its effect on peak concentration and dimensionless retention time is presented in Figure SI-8.2.a and b.
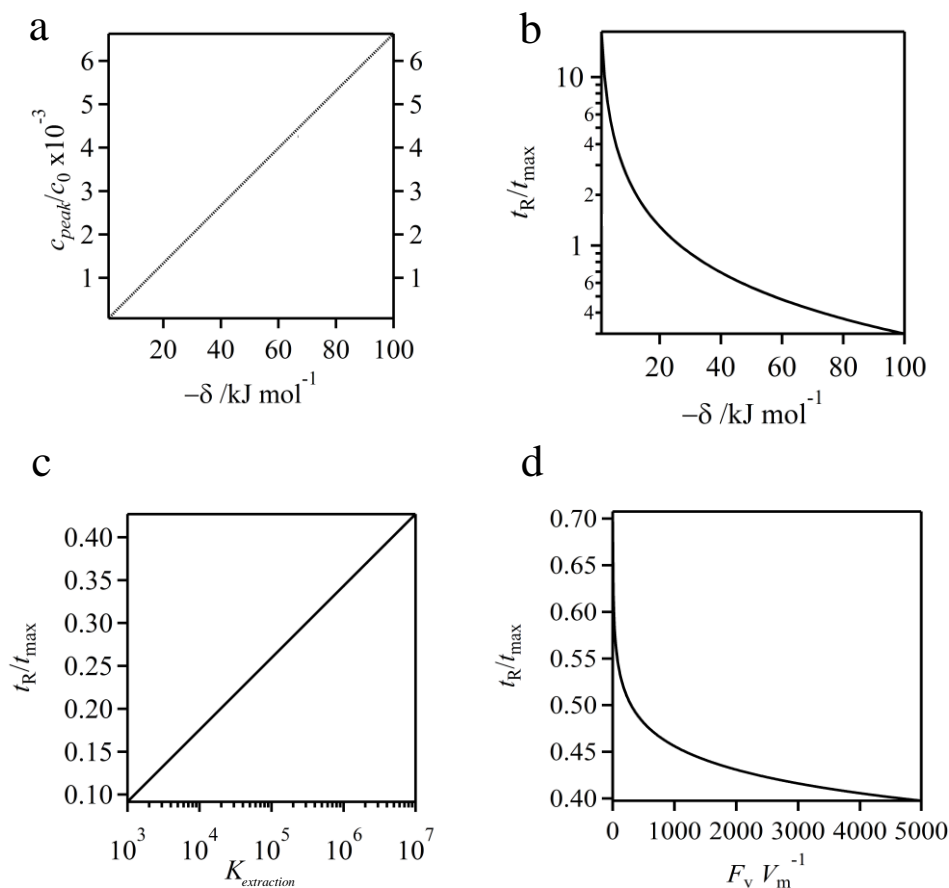
Figure SI-8.2. Analytical model of elution process. a) Effect of δ on peak concentration. b) Effect of δ on dimensionless retention time. c) Dependence of dimensionless retention time on $K_{extraction}$ s value (in logarithmic scale). d) Effect of flow rate factor $F_v \cdot V_m^{-1}$ on dimensionless retention time. Unless specified, $\delta = -68$ kJ· mol^{-1}, $K_{extraction} = 10^7$, $F_v \cdot V_m^{-1} = 2222.2$ (corresponds to 40 µL/h), $k_a = 10^6$ s^{-1} for all plots.

The analyte peak intensity is almost in linear relationship with δ for elution of hydrophobic species where the difference of solvation energy is in the kJ·mol^{-1} range (Hearn, M. T. W.; Aguilar, M. I. *J. Chromatogr.* **1987**, *397*, 47–70). In contrast, the extraction constant $K_{extraction}$ has minor influence on the peak intensity. It determines the retention time in such a way that t_R is a linear function with respect to log $K_{extraction}$ (Figure SI-8.2.c). Another parameter is the flow rate factor $F_v \cdot V_m^{-1}$ that shows the amount of mobile phase volume passing through the cell in time unit. This parameter is in logarithmic relationship with the retention time (Figure SI-8.2.d). However, it has a minor influence if the flow rate ratio is in relatively small range.

SI-9: Peptides identified in SPE-GEMS analysis of the myoglobin digest and its fractions collected after OFFGEL separation

A. 560 nM Myoglobin digest

m/z	z	Peptide sequence	retention time (n=3), t_{Rav}[1]
1553.8***	1	(R)NDIAAKYKELGFQG (-) [141-154][2, 3,4]	4.8
1139.8**	2	(K)ASEDLKKHGTVVLTALGGILKK(K) [58-79]	6.6
1570.9***	3	(K)YLEFISDAIIHVLHSKHPGDFGADAQGAMTKALELFRNDIAAK(Y) [104-146]	7.9
1362.8***	3	(K)HKIPIKYLEFISDAIIHVLHSKHPGDFGADAQGAMTK(A) [98-134]	8.3
1506.9*	1	(K)KHGTVVLTALGGILK(K) [64-78]	11.7
1157.1**	3	(K)HGTVVLTALGGILKKKGHHEAELKPLAQSHATK(H) [65-97]	14.4
1635.0*	1	(K)KHGTVVLTALGGILKK(K) [64-79]	15.3
1762.9***	2	(K)VEADIAGHGQEVLIRLFTGHPETLEKFDKFK(H) [18-48]	17.1
1139.8**	2	(K)ASEDLKKHGTVVLTALGGILKK(K) [58-79]	17.7
1532.8*	1	(K)YLEFISDAIIHVL(H) [104-116][5]	18.1
1135.2***	3	(K)ASEDLKKHGTVVLTALGGILKKKGHHEAELKP(L) [58-89]	18.5
1168.6**	2	(K)IPIKYLEFISDAIIHVLHSK(H) [100-119]	19.1
1479.5**	3	(K)GHHEAELKPLAQSHATKHKIPIKYLEFISDAIIHVLHSK(H) [81-119]	19.2
1301.2**	2	(K)HKIPIKYLEFISDAIIHVLHSK(H) [98-119]	21.6
1516.9***	3	(K)IPIKYLEFISDAIIHVLHSKHPGDFGADAQGAMTKALELFR(N) [100-140]	22.2

B. OFFGEL fraction with pH 5.9 diluted 5 times

		ESI MS		
m/z	*z*	*Peptide sequence*	pI	retention time (n=3), t_{Rav}[1]
1084.0***	3	(K)VEADIAGHGQEVLIRLFTGH PETLEKFDK(F) [18-46][3, 4]	4.97	2.7
1158.3***	2	(R)LFTGHPETLEKFDKFKHLK(T) [33-51]	8.45	2.9
969.2***	2	(R)LFTGHPETLEKFDKFK(H) [33-48]	6.76	3.2
1116.2***	2	(K)HPGDFGADAQGAMTKALELFR(N) [120-140]	5.38	3.5
1271.5*	1	(R)LFTGHPETLEK(F) [33-43]	5.40	4.1
1285.8***	2	(K)GHHEAELKPLAQSHATKHKIPIK(Y) [81-103]	8.53	4.7
1420.1**	2	(K)TEAEMKASEDLKKHGTVVLTALGGILK (K) [52-78]	6.44	8.5
1045.8**	3	(K)HPGDFGADAQGAMTKALELFRNDIAA KYK(E) [120-148]	6.76	10.4
1815.1***	1	(M)GLSDGEWQQVLNVWGK(V) [2-17][5]	4.37	11.6
1157.3**	3	(K)HGTVVLTALGGILKKKGHHEAELKPLA QSHATK(H) [65-97]	9.83	13.5
1168.8**	2	(K)IPIKYLEFISDAIIHVLHSK(H) [100-119]	6.92	15.6
1075.6**	2	(K)ASEDLKKHGTVVLTALGGILK(K) [58-78]	8.55	12.8
1378.7***	1	(K)HGTVVLTALGGILK(K) [65-78]	8.76	17.8
943.1*	2	(K)YLEFISDAIIHVLHSK(H) [104-119]	5.99	19.0
1273.9**	3	(K)IPIKYLEFISDAIIHVLHSKHPGDFGADA QGAMTK(A) [100-134]	6.27	19.1
1301.4**	2	(K)HKIPIKYLEFISDAIIHVLHSK(H) [98-119]	8.45	20.1
1123.5**	3	(K)YLEFISDAIIHVLHSKHPGDFGADAQGA MTK(A) [104-134]	5.74	22.4

C. OFFGEL fraction with pH 8.4 diluted 5 times

		ESI MS		
m/z	*z*	*Peptide sequence*	pI	retention time (n=3), t_{Rav}[1]
1124.2***	2	(K)KGHHEAELKPLAQSHATKHK(I) [80-99][3, 4]	9.53	3.1
1055.6***	2	(K)KKGHHEAELKPLAQSHATK(H) [79-97]	9.53	3.3
1853.9***	1	(K)GHHEAELKPLAQSHATK(H) [81-97]	7.03	4.6
1568.2**	2	(K)HPGDFGADAQGAMTKALELFRNDIAAK YK(E) [120-148]	6.76	9.3
1420.1**	2	(K)TEAEMKASEDLKKHGTVVLTALGGILK(K) [52-78]	6.44	10.0
1506.9**	1	(K)KHGTVVLTALGGILK(K) [64-78]	10.0	10.4
1157.3**	3	(K)HGTVVLTALGGILKKKGHHEAELKPLAQ SHATK(H) [65-97]	9.83	14.6
1139.8**	2	(K)ASEDLKKHGTVVLTALGGILKK(K) [58-79]	9.53	15.2
1022.3***	4	(K)HKIPIKYLEFISDAIIHVLHSKHPGDFGAD AQGAMTK(A) [98-134]	7.1	15.7
1075.6*	2	(K)ASEDLKKHGTVVLTALGGILK(K) [58-78]	8.55	16.7
1635.0**	1	(K)KHGTVVLTALGGILKK(K) [64-79]	10.30	18.3
1273.9**	3	(K)IPIKYLEFISDAIIHVLHSKHPGDFGADAQ GAMTK(A) [100-134]	6.27	18.9
1479.5**	3	(K)GHHEAELKPLAQSHATKHKIPIKYLEFISD AIIHVLHSK(H) [81-119]	8.38	19.2
1123.5**	3	(K)YLEFISDAIIHVLHSKHPGDFGADAQGAM TK(A) [104-134]	5.74	19.9
1301.4*	2	(K)HKIPIKYLEFISDAIIHVLHSK(H) [98-119]	8.45	20.2
1168.8**	2	(K)IPIKYLEFISDAIIHVLHSK(H) [100-119]	6.92	20.7

*-Peptide previously identified in corresponding ESI-MS control experiment with commercial ionization source.

**-Peptide not observed in the control ESI-MS experiment, but found also in SPE-GEMS analysis of two other samples (*e.g.* in whole digest or other OFFGEL fraction analysis, or in both cases).

***-Peptide observed only during SPE-GEMS analysis of current sample.

[1.]Presented values are the average retention times calculated from three replicates of each experiment

[2.](-) means that peptide is generated from a terminal of the protein.

[3] Presented sequences of identified peptides include the main amino acid sequence and the amino acids before and after the place of cleavage by trypsin in parentheses. Positions of the peptides in myoglobin are shown in square brackets.

[4.]Peptides presented in the black color are resulted from specific cleavage of myoglobin by trypsin.

[5.]Peptides shown in the red color are generated by semi-specific cleavage of myoglobin by trypsin, where only one end of peptide is formed by cleavage besides lysine or arginine residues. These sequences were identified by ESI MS/MS analysis (data not shown) using collision induced dissociation based on the theoretical data obtained with the use of *FindPept* tool on the ExPASy server (http://web.expasy.org/findpept/).

As can be concluded from the obtained results there is a difference in the observed ion charge states in control ESI-MS experiment and in SPE-GEMS analysis. In contrast with control experiments where the pH of the spraying solutions is ~2.8, the pH of spraying solution in SPE-GEMS analysis is only ~4.7 what leads to the formation of ions with smaller charge states ($m/z \leq 3$).

a 1 μM myoglobin tryptic digest

MALDI MS spectra

$M^+=748$

$M^+=942$

$M^+=1272$

$M^+=1607$

Int

m/z

b 1 μM myoglobin tryptic digest

ESI MS spectra

$M^{3+}=536.3$

$M^{2+}=636.3$

$M^{2+}=767.1$

$M^{2+}=804.1$

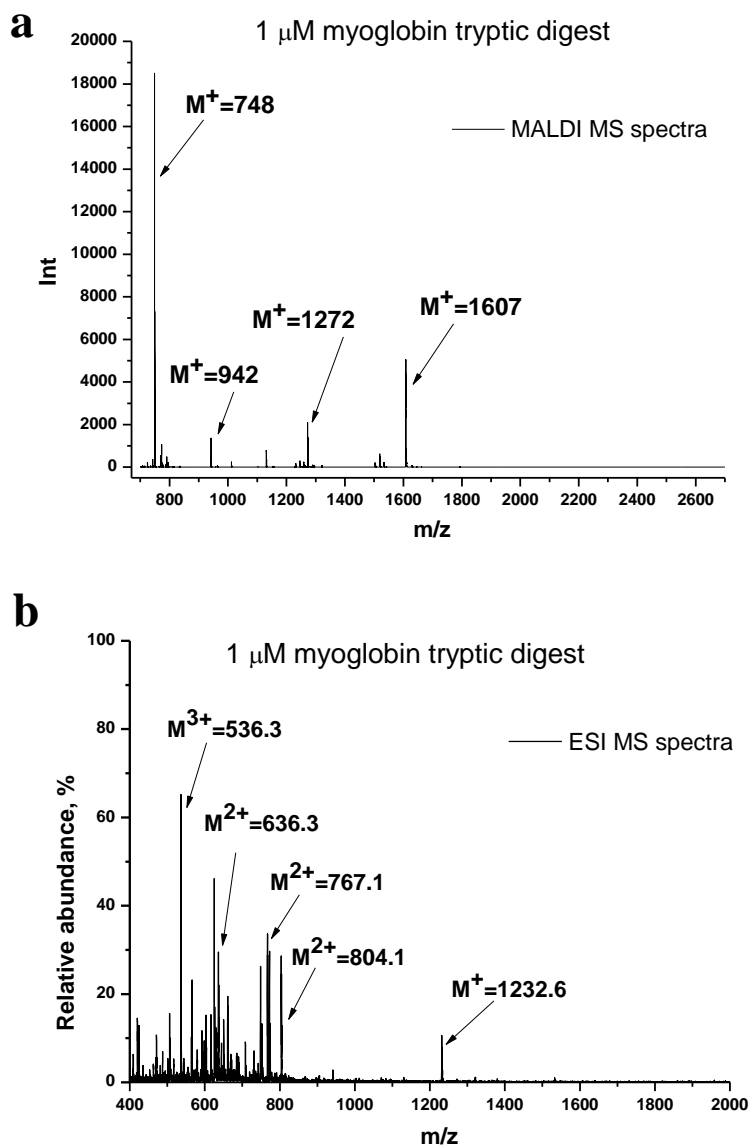$M^+=1232.6$

Relative abundance, %

m/z

Figure SI-10. MS spectra of 1 μM solution of myoglobin digest: a) MALDI-MS and b) ESI-MS spectrum. For MALDI-MS matrix solution was composed of 10 mg/mL solution of 2,5-dihydroxybenzoic acid in 50% water and 50% acetonitrile. Ions marked on the plots correspond to the peptides presented in Table SI-10.

List of peptides identified in control MALDI and ESI-MS experiments are presented below in Table SI-10. Sequences for peptides are proposed based on the comparison of the observed molecular

weights with the theoretical ones from the databases using *FindPept* tool on the ExPASy server (http://web.expasy.org/findpept/).

Table SI-10. Peptides observed during MALDI and ESI-MS analysis of 1 µM myoglobin tryptic digest solution.

MALDI MS			ESI MS		
m/z	*z*	*Peptide sequence*	*m/z*	*z*	*Peptide sequence*
748	1	(K)ALELFR(N) [135-140][1, 2]	409.6	4	(K)KHGTVVLTALGGILKK(K) [64-79]
790	1	(K)ASEDLKK(H) [58-64]	565.7	2	(K)GHHEAELKPL(A) [81-90][3]
942	1	(K)YKELGFQG(-) [147-154][4]	636.3	2	(R)LFTGHPETLEK(F) [33-43]
1131	1	(K)GHHEAELKPL(A) [81-90]	650.3	1	(K)ELGFQG(-) [149-154]
1232	1	GLSDGEWQQVL(N) [2-12]	708.4	1	(K)TEAEMK(A) [52-57]
1272	1	(R)LFTGHPETLEK(F) [33-43]	748.4	1	(K)ALELFR(N) [135-140]
1502	1	(K)HPGDFGADAQGAMTK(A) [120-134]	754.1	2	(K)KHGTVVLTALGGILK(K) [64-78]
1533	1	(K)YLEFISDAIIHVL(H) [104-116]	767.1	2	(K)YLEFISDAIIHVL(H) [104-116]
1606	1	(K)VEADIAGHGQEVLIR(L) [18-32]	536.3	3	(K)VEADIAGHGQEVLIR(L) [18-32]
			804.1	2	
			941.5	1	(K)YKELGFQG(-) [147-154]
			616.2	2	GLSDGEWQQVL(N) [2-12]
			1232.6	1	

[1.]Presented sequences of identified peptides include the main amino acid sequence and the amino acids before and after the place of cleavage by trypsin in parentheses. Positions of the peptides in myoglobin are shown in square brackets.

[2.]Peptides presented in the black color are resulted from specific cleavage of myoglobin by trypsin.

[3.]Peptides shown in the red color are generated by semi-specific cleavage of myoglobin by trypsin, where only one end of peptide is formed by cleavage besides lysine or arginine residues. These sequences were identified by ESI MS/MS analysis (data not shown) using collision induced dissociation based on the theoretical data obtained with a use of *FindPept* tool on the ExPASy server (http://web.expasy.org/findpept/).

[4.](-) means that peptide is generated from a terminal of the protein.

SI-11: MALDI and ESI-MS analysis of fractions collected after OFFGEL separation of the myoglobin digest solution without preconcentration using a commercial ionization source
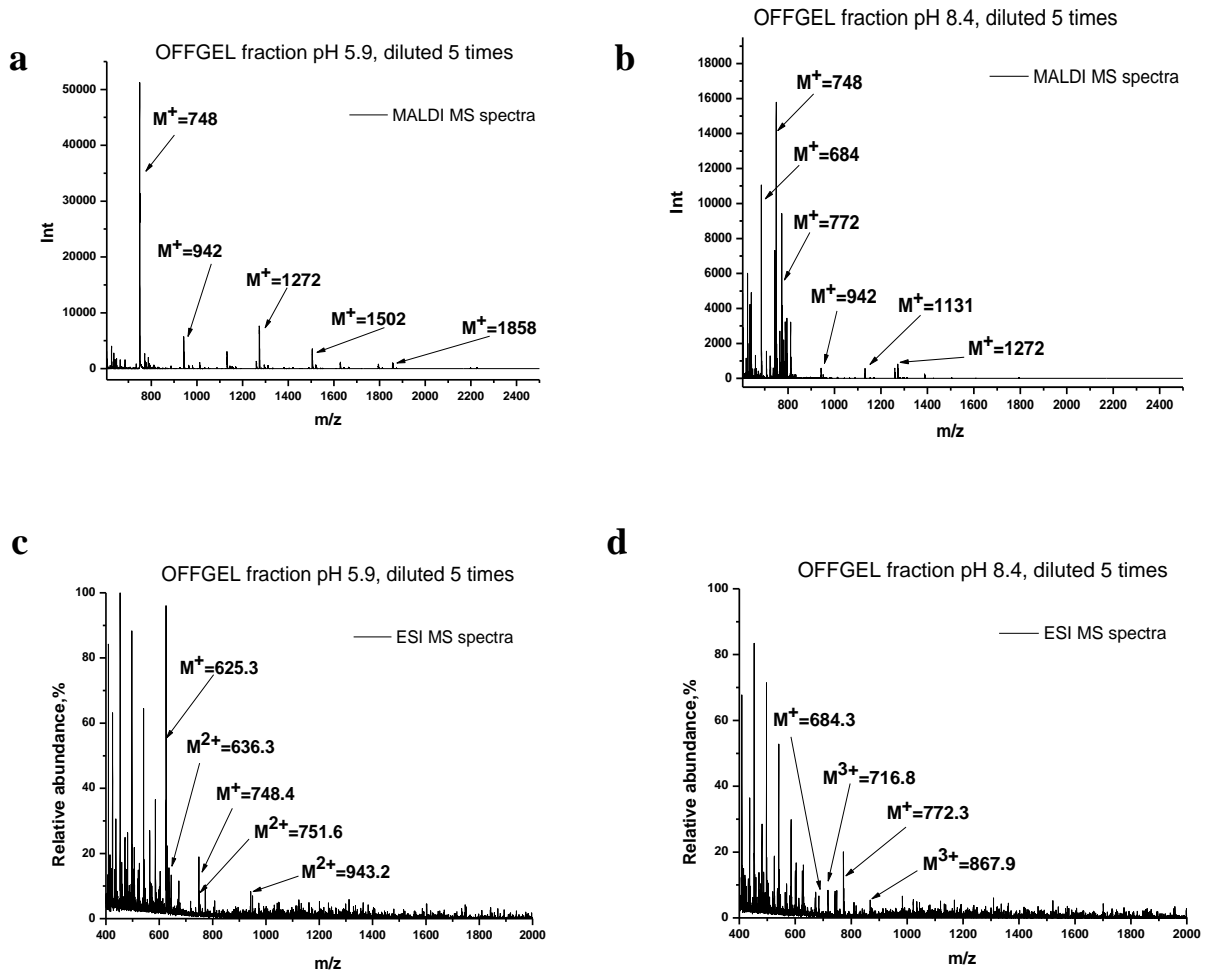

Figure SI-11. MS spectra of two fractions collected after OFFGEL separation of myoglobin digest. a), b) MALDI-MS spectra of fractions with pH 5.9 and 8.4, respectively. c), d) ESI-MS spectra of fractions with pH 5.9 and 8.4, respectively. Both fractions were diluted 5 times prior to the analysis. For MALDI-MS matrix solution was composed of 10 mg/mL solution of 2,5-dihydroxybenzoic acid in 50% water and 50% acetonitrile. Ions marked on the plots correspond to the peptides presented in Table SI-11 A and B.

List of peptides identified in control MALDI and ESI-MS experiments of OFFGEL fractions are presented below in Table SI-11. Sequences for peptides are proposed based on the comparison of the ob-

served molecular weights with the theoretical ones from databases using *FindPept* tool on the ExPASy

server (http://web.expasy.org/findpept/). Theoretical pI values for peptides are calculated using *Compute*

pI/MW tool from ExPASy server (http://web.expasy.org/findpept/).

Table SI-11. Peptides observed during MALDI and ESI-MS analysis of two fractions collected after OFFGEL separation of myoglobin digest

A. OFFGEL fraction with pH 5.9 diluted 5 times

MALDI MS				ESI MS			
m/z	*z*	*Peptide sequence*	pI	*m/z*	*z*	*Peptide sequence*	pI
625	1	(K)HGTVVL(T) [65-70][1, 2]	6.74	471.3	2	(K)YKELGFQG(-) [147-154][3, 4]	6.00
748	1	(K)ALELFR(N) [135-140]	6.05	625.3	1	(K)HGTVVL(T) [65-70]	6.74
790	1	(K)ASEDLKK(H) [58-64]	6.11	636.3	2	(R)LFTGHPETLEK(F) [33-43]	5.4
942	1	(K)YKELGFQG(-) [147-154]	6.00	748.4	1	(K)ALELFR(N) [135-140]	6.05
1131	1	(K)GHHEAELKPL(A) [81-90]	6.00	751.3	2	(K)HPGDFGADAQGAMTK(A) [120-134]	5.21
1272	1	(R)LFTGHPETLEK(F) [33-43]	5.40	943.2	2	(K)YLEFISDAIIHVLHSK(H) [104-119]	5.99
1502	1	(K)HPGDFGADAQGAMTK(A) [120-134]	5.21				
1858	1	(K)HLKTEAEMKASEDLKK(H) [49-64]	6.77				

B. OFFGEL fraction with pH 8.4 diluted 5 times

MALDI MS				ESI MS			
m/z	*z*	*Peptide sequence*	pI	*m/z*	*z*	*Peptide sequence*	pI
684	1	(K)FDKFK(H) [44-48][1, 3]	8.59	684.3	1	(K)FDKFK(H) [44-48]	8.59
748	1	(K)ALELFR(N) [135-140]	6.05	716.8	3	(K)ASEDLKKHGTVVLTALGGILK(K) [58-78]	8.55
772	1	(L)TALGGILK(K) [71-78][2]	8.41	748.4	1	(K)ALELFR(N) [135-140]	6.05
942	1	(K)YKELGFQG(-) [147-154][4]	6.00	772.3	1	(L)TALGGILK(K) [71-78]	8.41
1131	1	(K)GHHEAELKPL(A) [81-90]	6.00	867.9	3	(K)HKIPIKYLEFISDAIIHVLHSK(H) [98-119]	
1272	1	(R)LFTGHPETLEK(F) [33-43]	5.40				

In contrast with the results for the whole unprocessed digest few peptides belonging to the myoglobin were identified on the control ESI-MS spectra of both OFFGEL fractions. At the same time several intensive peaks (m/z= 409.3, 453.2, 495.3, 539.3, 583.4, 628.3 Da) which do not correspond to the myoglobin were clearly observed. As Δ m/z between these peaks remains the same and is equal to 44 Da, while the charge state z of all these peaks is equal to 1, these is a high probability that these peaks are related to the polymer fragments which contaminated the OFFGEL fractions at the collection step. The presence of such contamination masks the signal from the peptides of interest in control ESI-MS experiment. During SPE-GEMS analysis of OFFGEL fractions these contamination peaks were not observed due to the purification effect.

In case of the analysis of OFFGEL fraction with pH 5.9 peptides with theoretical pI values in the range 5.9±0.9 were identified. This result is typical for OFFGEL separation due to the absence of sharp pH borders in IEF gels. Some of these peptides (MW= 748, 942, 1131, 1272 Da) were also observed with lower intensities on the spectra of the OFFGEL fraction with pH 8.4 together with only 2 peptides possessing pI values in the range of 8.5. These listed peptides also clearly appear on the control spectra of whole myoglobin digest and are presented in a wide range of the wells in different amounts (the highest in the wells with pHs matching with pIs of peptides, data not shown) after OFFGEL separation due to their high abundance among the products of myoglobin tryptic digestion. To decrease the concentration

of these peptides in inappropriate wells the quality of OFFGEL separation could be further increased by prolonging experimental time (in current work the OFFGEL separation lasted for 18 hours).

Annex: Numerical simulations

The numerical model of gradient elution inside a SPE-GEMS microchip was build up using commercially available software package COMSOL Multiphysics (version 3.5a) operating on MacPro with four 2.66 GHz CPU and 9.8 Gb RAM under Linux Ubuntu environment. The modeling was performed by numerical resolution of steady-state Navier-Stokes and transient diffusion/convection equations in a two-dimensional computational domain. The solution was computed in a sequential mode, *i.e.* calculation of diffusion/convection equation system was performed on top of the computed fluid velocity field by using "Store solution" option assuming that fluid's properties are not affected by the change of concentration of dissolved species and the eluent content. More details are presented in the main manuscript.
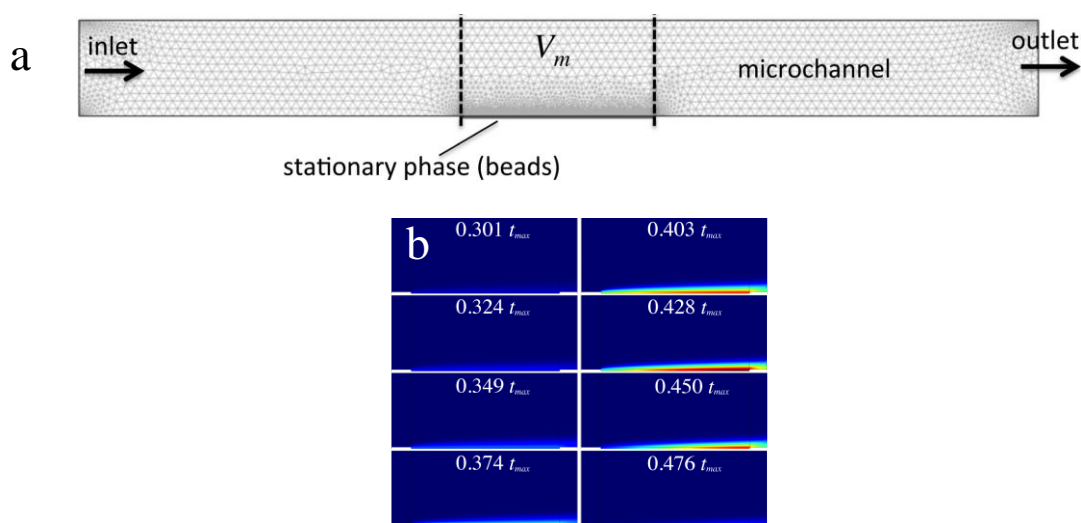
Figure SI-Annex. FEM modeling of elution process in the microchannel. a) Schematic representation of computational domain and mesh implemented for calculations. b) Magnified view on concentration distributions within the microchannel depicting evolution of desorption process.

The analyte transport within the microchannel is shown on schematic representation in Figure SI-Annex.a. As shown on color maps in Figure SI-Annex.b, the desorption of analyte species into eluent occurs just in a thin layer near the stationary phase because the tangential convective mass transport is fast enough in comparison with relatively slow diffusion along the vertical axis of a microchannel. More

details of FEM simulation procedure, geometrical parameters of computational domain, meshing, initial

and boundary settings are presented below in generated Comsol report.

COMSOL Model Report
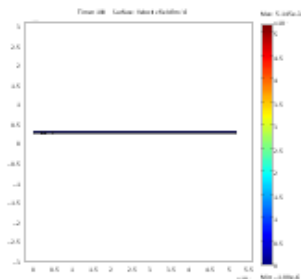
1. Table of Contents

2. Model Properties

Property	Value
Model name	
Author	
Company	
Department	
Reference	
URL	
Saved date	Dec 18, 2012 10:38:45 AM
Creation date	Jul 25, 2012 12:06:20 PM
COMSOL version	COMSOL 3.5.0.603

File name: /home/dmitry/Desktop/elution model.mph

Application modes and modules used in this model:

- Geom1 (2D)
    - Diffusion (Chemical Engineering Module)
    - Convection and Diffusion (Chemical Engineering Module)
    - Incompressible Navier-Stokes

3. Constants

Name	Expression	Value	Description
cs0	1[mmol/l]		initial conc in stationary phase

Ds	1e-10[m^2/s]		diffusion coefficient in stationary phase
D	1e-10[m^2/s]		diffusion coefficient in microchip
ka	1e6[1/s]		adsorpt coefficient
VF	40[ul/h]		volumic flowrate
CrS	50[um]*100[um]		cross-sectional area of microchannel
R	8.31[J/mol/K]		gas const
T	298[K]		temperature
delta	-68000[J/mol]		delta, i.e. dGoil-dGwater
beta	0.01[1/s]		composition change rate
Kextr	10^7		adsorption const from water to Mbs

4. Global Expressions

Name	Expression	Unit	Description
dGp	-R*T*log(Kextr)-delta*beta*t	J/mol	dG of the partition
kd	ka*exp(dGp/(R*T))	1/s	kd expression
Flux	kd*cs-ka*c	mol/(m^3*s)	

5. Geometry

Number of geometries: 1

5.1. Geom1
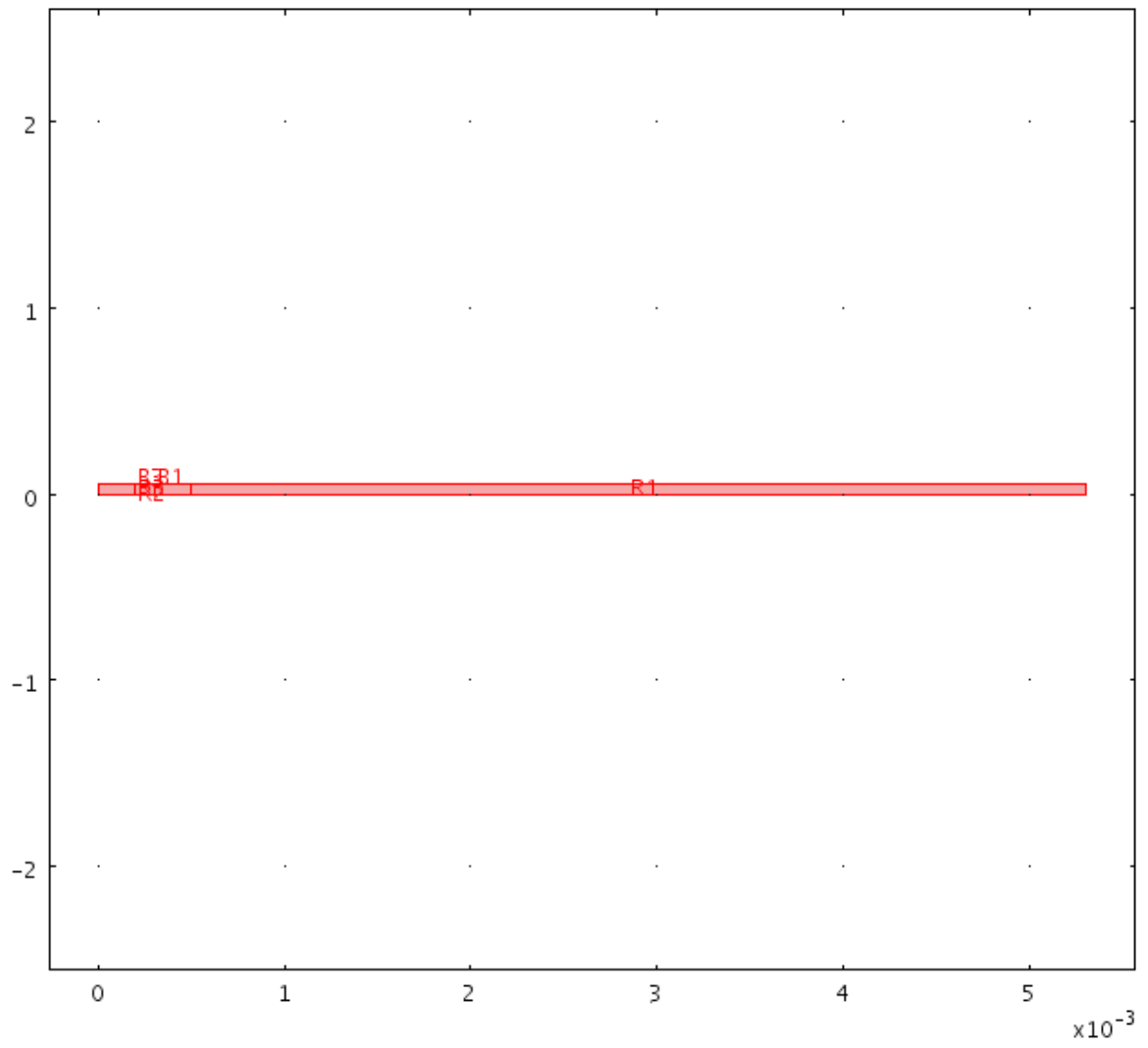
5.1.1. Point mode
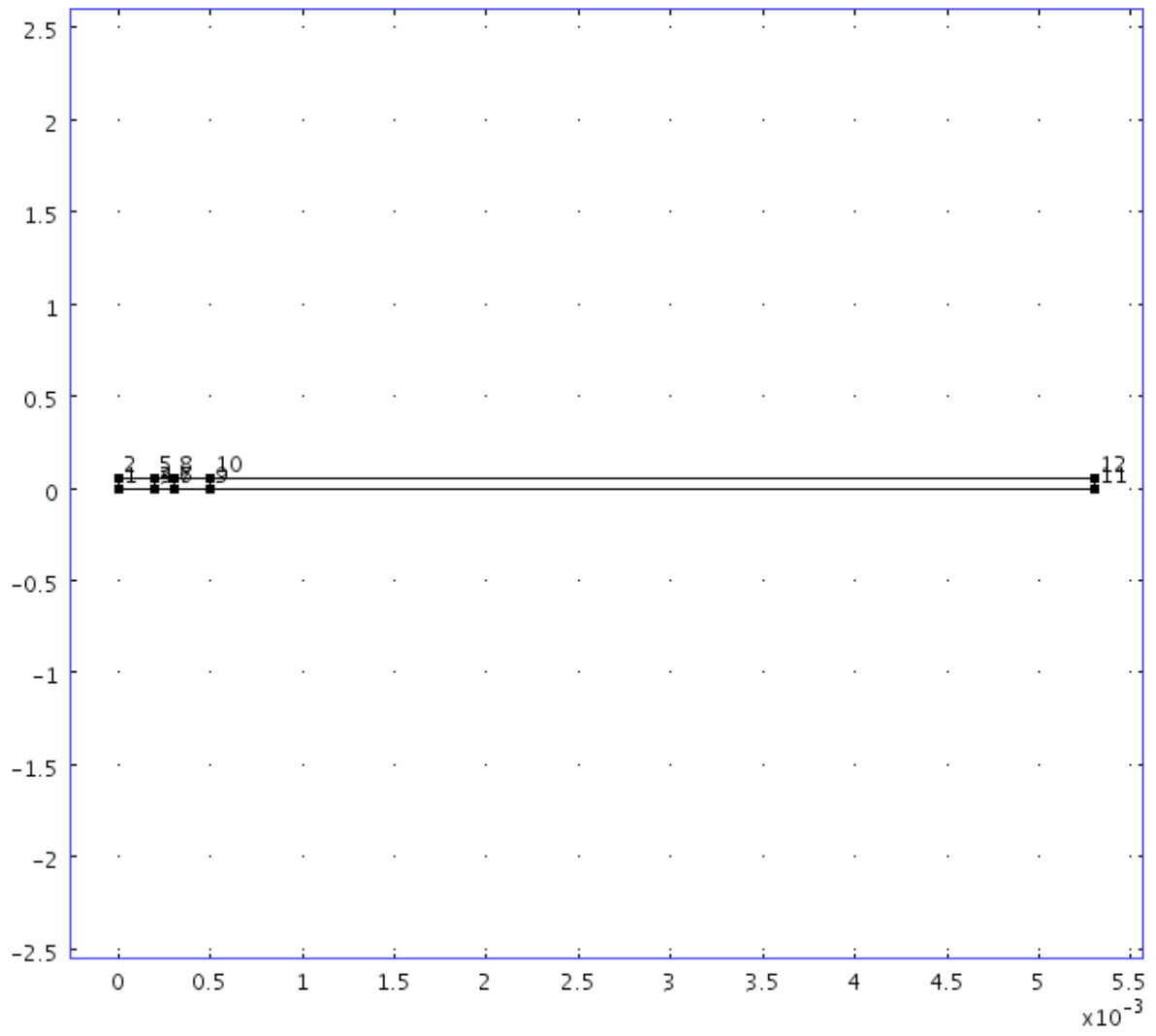
5.1.2. Boundary mode
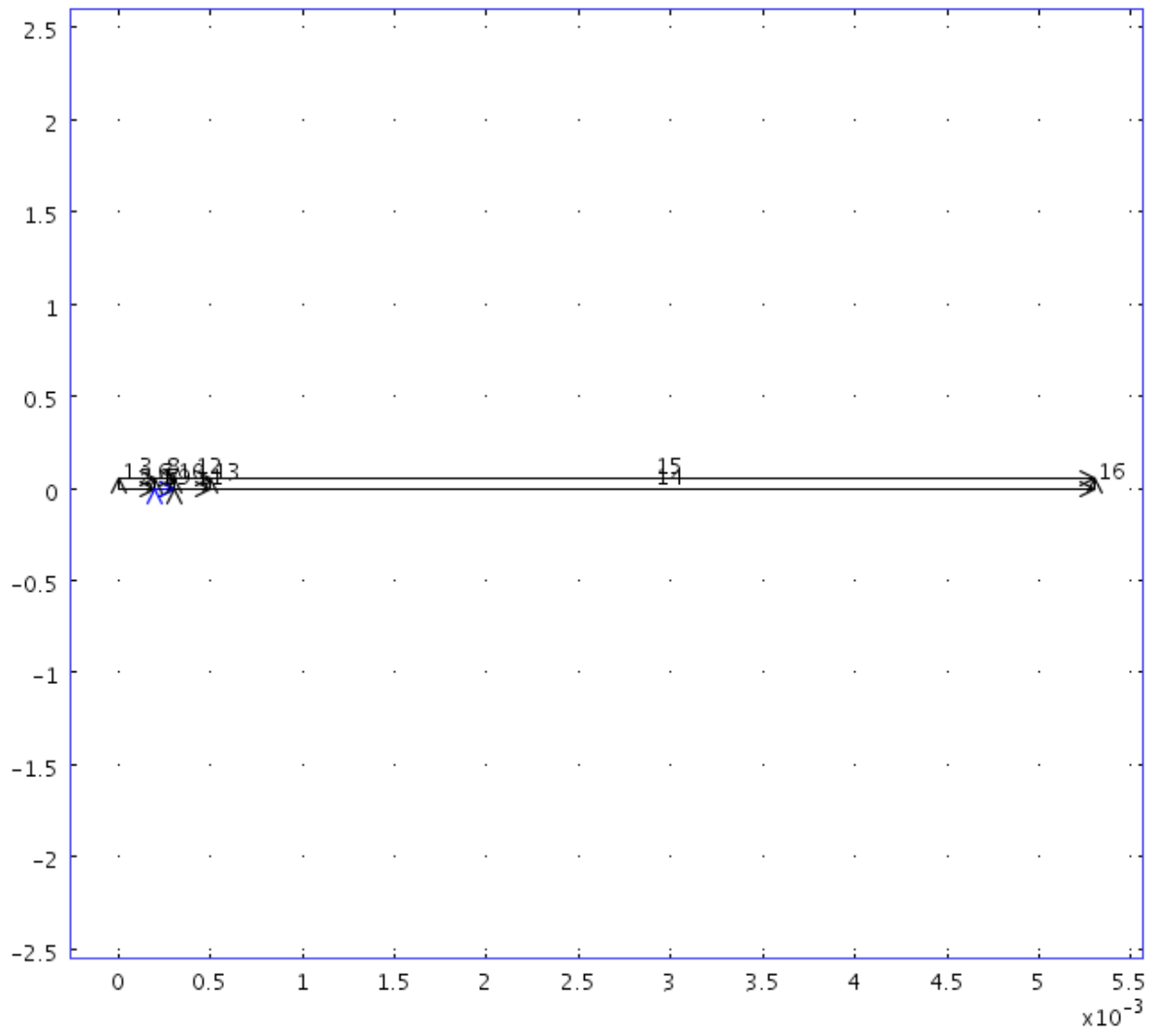
5.1.3. Subdomain mode
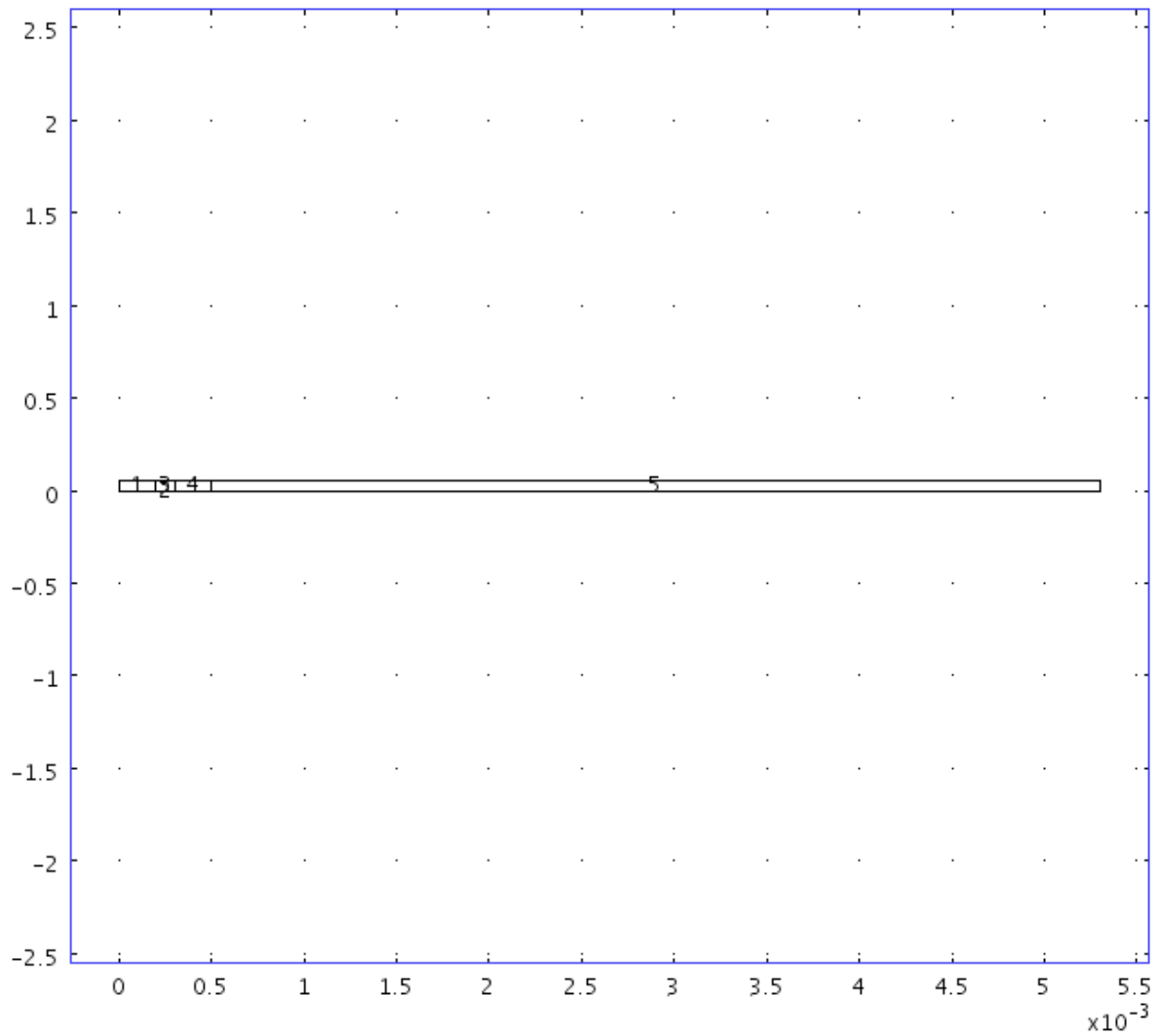
6. Geom1

Space dimensions: 2D

Independent variables: x, y, z

6.1. Mesh

6.1.1. Mesh Statistics

Number of degrees of freedom	502528
Number of mesh points	44386
Number of elements	84961
Triangular	84961
Quadrilateral	0
Number of boundary elements	4948
Number of vertex elements	12
Minimum element quality	0.778
Element area ratio	0
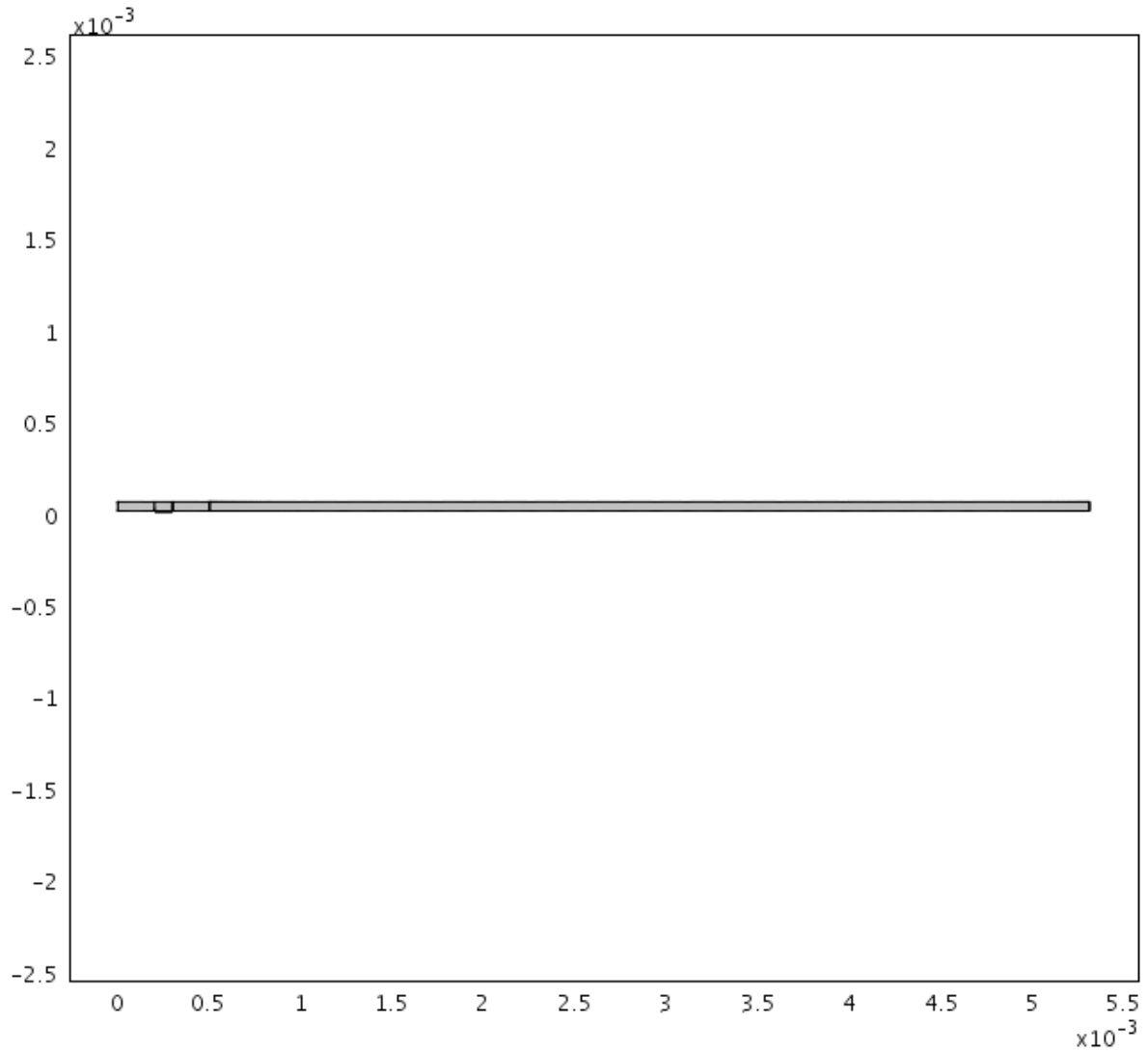
6.2. Application Mode: Diffusion (chdi)

Application mode type: Diffusion (Chemical Engineering Module)

Application mode name: chdi

6.2.1. Application Mode Properties

Property	Value
Default element type	Lagrange - Quadratic
Analysis type	Transient
Equilibrium assumption	Off
Frame	Frame (ref)
Weak constraints	Off
Constraint type	Ideal

6.2.2. Variables

Dependent variables: cs

Shape functions: shlag(2,'cs')

Interior boundaries not active

6.2.3. Boundary Settings

Boundary		4, 7	5, 9
Type		Insulation/Symmetry	Insulation/Symmetry
Inward flux (N)	mol/(m$^2\cdot$s)	**-Flux**	0

6.2.4. Subdomain Settings

Subdomain		2
Diffusion coefficient (D)	m^2/s	**Ds**
Reaction rate (R)	mol/(m$^3\cdot$s)	**-Flux**

Subdomain initial value		2
Concentration, cs (cs)	mol/m^3	cs0

6.3. Application Mode: Convection and Diffusion (chcd)

Application mode type: Convection and Diffusion (Chemical Engineering Module)

Application mode name: chcd

6.3.1. Application Mode Properties

Property	Value
Default element type	Lagrange - Quadratic
Analysis type	Transient
Equation form	Non-conservative
Equilibrium assumption	Off
Frame	Frame (ref)
Weak constraints	Off
Constraint type	Ideal

6.3.2. Variables

Dependent variables: c

Shape functions: shlag(2,'c')

Interior boundaries active

6.3.3. Boundary Settings

Boundary		1	2-5, 8-9, 11-12, 14-15	6, 10, 13
Type		Concentration	Insulation/Symmetry	Continuity
Inward flux (N)	mol/(m$^2\cdot$s)	0	0	0

Boundary		7	16
Type		Continuity	Convective flux
Inward flux (N)	mol/(m$^2\cdot$s)	**Flux**	0

6.3.4. Subdomain Settings

Subdomain		1, 3-5	2
Diffusion coefficient (D)	m2/s	**D**	**Ds**
Reaction rate (R)	mol/(m3·s)	0	**Flux**
x-velocity (u)	m/s	**u**	0
y-velocity (v)	m/s	**v**	0

6.4. Application Mode: Incompressible Navier-Stokes (ns)

Application mode type: Incompressible Navier-Stokes

Application mode name: ns

6.4.1. Scalar Variables

Name	Variable	Value	Unit	Description
visc_vel_fact	visc_vel_fact_ns	10	1	Viscous velocity factor

6.4.2. Application Mode Properties

Property	Value
Default element type	Lagrange - P_2 P_1
Analysis type	Stationary
Corner smoothing	Off
Frame	Frame (ref)
Weak constraints	Off
Constraint type	Ideal

6.4.3. Variables

Dependent variables: u, v, p, nxw, nyw

Shape functions: shlag(2,'u'), shlag(2,'v'), shlag(1,'p')

Interior boundaries not active

6.4.4. Boundary Settings

Boundary		1	2-3, 7-8, 11-12, 14-15	16
Type		Inlet	Wall	Outlet
Normal inflow velocity (U0in)	m/s	**VF/CrS**	1	1

6.4.5. Subdomain Settings

Subdomain		1, 3-5
Integration order (gporder)		**4 4 2**
Constraint order (cporder)		**2 2 1**
Density (rho)	kg/m3	**1000**
Dynamic viscosity (eta)	Pa·s	**0.01**

7. Solver Settings

Solve using a script: off

Analysis type	Transient
Auto select solver	On
Solver	Time dependent
Solution form	Automatic
Symmetric	auto
Adaptive mesh refinement	Off
Optimization/Sensitivity	Off
Plot while solving	Off

7.1. Direct (UMFPACK)

Solver type: Linear system solver

Parameter	Value
Pivot threshold	0.1
Memory allocation factor	0.7

7.2. Time Stepping

Parameter	Value
Times	range(0,0.1,100)
Relative tolerance	1e-5
Absolute tolerance	1e-6
Times to store in output	Time steps from solver
Time steps taken by solver	Free
Maximum BDF order	5
Singular mass matrix	Maybe
Consistent initialization of DAE systems	Backward Euler
Error estimation strategy	Include algebraic
Allow complex numbers	Off

7.3. Advanced

Parameter	Value
Constraint handling method	Elimination
Null-space function	Automatic
Automatic assembly block size	On
Assembly block size	1000
Use Hermitian transpose of constraint matrix and in symmetry detection	Off
Use complex functions with real input	Off
Stop if error due to undefined operation	On
Store solution on file	Off
Type of scaling	Automatic
Manual scaling	
Row equilibration	On
Manual control of reassembly	Off
Load constant	On
Constraint constant	On
Mass constant	On
Damping (mass) constant	On

Jacobian constant	On
Constraint Jacobian constant	On

8. Postprocessing

Time=100   Surface: Velocity field [m/s]   Max: 5.145e-3

Min: −1.00e−6
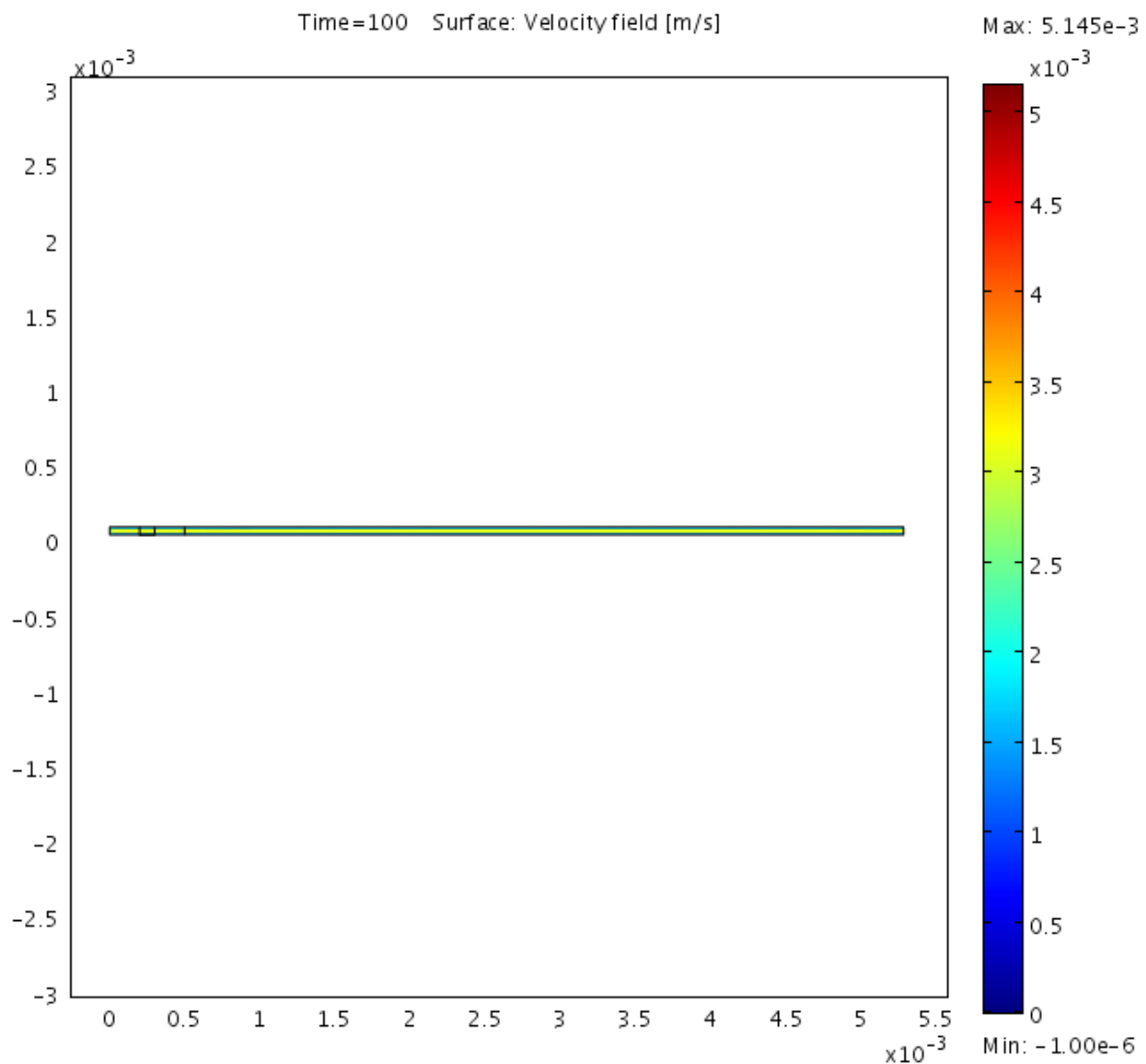
9. Variables

9.1. Boundary

9.1.1. Boundary 1-3, 6, 8, 10-16

Name	Description	Unit	Expression
ndflux_cs_chdi	Normal diffusive flux, cs	mol/(m^2*s)	
ndflux_c_chcd	Normal diffusive flux, c	mol/(m^2*s)	nx_chcd * dflux_c_x_chcd+ny_chcd * dflux_c_y_chcd
ncflux_c_chcd	Normal convective flux, c	mol/(m^2*s)	nx_chcd * cflux_c_x_chcd+ny_chcd * cflux_c_y_chcd
ntflux_c_chcd	Normal total flux, c	mol/(m^2*s)	nx_chcd * tflux_c_x_chcd+ny_chcd * tflux_c_y_chcd
K_x_ns	Viscous force per area, x component	Pa	eta_ns * (2 * nx_ns * ux+ny_ns * (uy+vx))
T_x_ns	Total force per area, x component	Pa	-nx_ns * p+2 * nx_ns * eta_ns * ux+ny_ns * eta_ns * (uy+vx)

Name	Description	Unit	Expression
K_y_ns	Viscous force per area, y component	Pa	eta_ns * (nx_ns * (vx+uy)+2 * ny_ns * vy)
T_y_ns	Total force per area, y component	Pa	-ny_ns * p+nx_ns * eta_ns * (vx+uy)+2 * ny_ns * eta_ns * vy

9.1.2. Boundary 4-5, 9

Name	Description	Unit	Expression
ndflux_cs_chdi	Normal diffusive flux, cs	mol/(m^2*s)	nx_chdi * dflux_cs_x_chdi+ny_chdi * dflux_cs_y_chdi
ndflux_c_chcd	Normal diffusive flux, c	mol/(m^2*s)	nx_chcd * dflux_c_x_chcd+ny_chcd * dflux_c_y_chcd
ncflux_c_chcd	Normal convective flux, c	mol/(m^2*s)	nx_chcd * cflux_c_x_chcd+ny_chcd * cflux_c_y_chcd
ntflux_c_chcd	Normal total flux, c	mol/(m^2*s)	nx_chcd * tflux_c_x_chcd+ny_chcd * tflux_c_y_chcd
K_x_ns	Viscous force per area, x component	Pa	
T_x_ns	Total force per area, x component	Pa	
K_y_ns	Viscous force per area, y component	Pa	
T_y_ns	Total force per area, y component	Pa	

9.1.3. Boundary 7

Name	Description	Unit	Expression
ndflux_cs_chdi	Normal diffusive flux, cs	mol/(m^2*s)	nx_chdi * dflux_cs_x_chdi+ny_chdi * dflux_cs_y_chdi
ndflux_c_chcd	Normal diffusive flux, c	mol/(m^2*s)	nx_chcd * dflux_c_x_chcd+ny_chcd * dflux_c_y_chcd
ncflux_c_chcd	Normal convective flux, c	mol/(m^2*s)	nx_chcd * cflux_c_x_chcd+ny_chcd * cflux_c_y_chcd
ntflux_c_chcd	Normal total flux, c	mol/(m^2*s)	nx_chcd * tflux_c_x_chcd+ny_chcd * tflux_c_y_chcd
K_x_ns	Viscous force per area, x component	Pa	eta_ns * (2 * nx_ns * ux+ny_ns * (uy+vx))
T_x_ns	Total force per area, x component	Pa	-nx_ns * p+2 * nx_ns * eta_ns * ux+ny_ns * eta_ns * (uy+vx)
K_y_ns	Viscous force per area, y component	Pa	eta_ns * (nx_ns * (vx+uy)+2 * ny_ns * vy)
T_y_ns	Total force per area, y component	Pa	-ny_ns * p+nx_ns * eta_ns * (vx+uy)+2 * ny_ns * eta_ns * vy

9.2. Subdomain

9.2.1. Subdomain 1, 3-5

Name	Description	Unit	Expression
grad_cs_x_chdi	Concentration gradient, cs, x component	mol/m^4	

dflux_cs_x_chdi	Diffusive flux, cs, x component	mol/(m^2*s)	
grad_cs_y_chdi	Concentration gradient, cs, y component	mol/m^4	
dflux_cs_y_chdi	Diffusive flux, cs, y component	mol/(m^2*s)	
grad_cs_chdi	Concentration gradient, cs	mol/m^4	
dflux_cs_chdi	Diffusive flux, cs	mol/(m^2*s)	
grad_c_x_chcd	Concentration gradient, c, x component	mol/m^4	cx
dflux_c_x_chcd	Diffusive flux, c, x component	mol/(m^2*s)	-Dxx_c_chcd * cx-Dxy_c_chcd * cy
cflux_c_x_chcd	Convective flux, c, x component	mol/(m^2*s)	c * u_c_chcd
tflux_c_x_chcd	Total flux, c, x component	mol/(m^2*s)	dflux_c_x_chcd+cflux_c_x_chcd
grad_c_y_chcd	Concentration gradient, c, y component	mol/m^4	cy
dflux_c_y_chcd	Diffusive flux, c, y component	mol/(m^2*s)	-Dyx_c_chcd * cx-Dyy_c_chcd * cy
cflux_c_y_chcd	Convective flux, c, y component	mol/(m^2*s)	c * v_c_chcd
tflux_c_y_chcd	Total flux, c, y component	mol/(m^2*s)	dflux_c_y_chcd+cflux_c_y_chcd
beta_c_x_chcd	Convective field, c, x component	m/s	u_c_chcd
beta_c_y_chcd	Convective field, c, y component	m/s	v_c_chcd
grad_c_chcd	Concentration gradient, c	mol/m^4	sqrt(grad_c_x_chcd^2+grad_c_y_chcd^2)
dflux_c_chcd	Diffusive flux, c	mol/(m^2*s)	sqrt(dflux_c_x_chcd^2+dflux_c_y_chcd^2)
cflux_c_chcd	Convective flux, c	mol/(m^2*s)	sqrt(cflux_c_x_chcd^2+cflux_c_y_chcd^2)
tflux_c_chcd	Total flux, c	mol/(m^2*s)	sqrt(tflux_c_x_chcd^2+tflux_c_y_chcd^2)
cellPe_c_chcd	Cell Peclet number, c	1	h * sqrt(beta_c_x_chcd^2+beta_c_y_chcd^2)/Dm_c_chcd
Dm_c_chcd	Mean diffusion coefficient, c	m^2/s	(Dxx_c_chcd * u_c_chcd^2+Dxy_c_chcd * u_c_chcd * v_c_chcd+Dyx_c_chcd * v_c_chcd * u_c_chcd+Dyy_c_chcd * v_c_chcd^2)/(u_c_chcd^2+v_c_chcd^2+eps)
res_c_chcd	Equation residual for c	mol/(m^3*s)	-Dxx_c_chcd * cxx-Dxy_c_chcd * cxy+cx * u_c_chcd-Dyx_c_chcd * cyx-Dyy_c_chcd * cyy+cy * v_c_chcd-R_c_chcd
res_sc_c_chcd	Shock capturing residual for c	mol/(m^3*s)	cx * u_c_chcd+cy * v_c_chcd-R_c_chcd
da_c_chcd	Total time scale factor, c	1	Dts_c_chcd
U_ns	Velocity field	m/s	sqrt(u^2+v^2)
V_ns	Vorticity	1/s	vx-uy
divU_ns	Divergence of	1/s	ux+vy

cellRe_ns	Cell Reynolds number	1	rho_ns * U_ns * h/eta_ns
res_u_ns	Equation residual for u	N/m^3	rho_ns * (u * ux+v * uy)+px-F_x_ns-eta_ns * (2 * uxx+uyy+vxy)
res_v_ns	Equation residual for v	N/m^3	rho_ns * (u * vx+v * vy)+py-F_y_ns-eta_ns * (vxx+uyx+2 * vyy)
beta_x_ns	Convective field, x component	kg/(m^2*s)	rho_ns * u
beta_y_ns	Convective field, y component	kg/(m^2*s)	rho_ns * v
Dm_ns	Mean diffusion coefficient	Pa*s	eta_ns
da_ns	Total time scale factor	kg/m^3	rho_ns
taum_ns	GLS time-scale	m^3*s/kg	nojac(1/max(2 * rho_ns * sqrt(emetric(u,v)),48 * eta_ns/h^2))
tauc_ns	GLS time-scale	m^2/s	0.5 * nojac(if(u^2+v^2
res_p_ns	Equation residual for p	kg/(m^3*s)	rho_ns * divU_ns

9.2.2. Subdomain 2

Name	Description	Unit	Expression
grad_cs_x_chdi	Concentration gradient, cs, x component	mol/m^4	csx
dflux_cs_x_chdi	Diffusive flux, cs, x component	mol/(m^2*s)	-Dxx_cs_chdi * csx-Dxy_cs_chdi * csy
grad_cs_y_chdi	Concentration gradient, cs, y component	mol/m^4	csy
dflux_cs_y_chdi	Diffusive flux, cs, y component	mol/(m^2*s)	-Dyx_cs_chdi * csx-Dyy_cs_chdi * csy
grad_cs_chdi	Concentration gradient, cs	mol/m^4	sqrt(grad_cs_x_chdi^2+grad_cs_y_chdi^2)
dflux_cs_chdi	Diffusive flux, cs	mol/(m^2*s)	sqrt(dflux_cs_x_chdi^2+dflux_cs_y_chdi^2)
grad_c_x_chcd	Concentration gradient, c, x component	mol/m^4	cx
dflux_c_x_chcd	Diffusive flux, c, x component	mol/(m^2*s)	-Dxx_c_chcd * cx-Dxy_c_chcd * cy
cflux_c_x_chcd	Convective flux, c, x component	mol/(m^2*s)	c * u_c_chcd
tflux_c_x_chcd	Total flux, c, x component	mol/(m^2*s)	dflux_c_x_chcd+cflux_c_x_chcd
grad_c_y_chcd	Concentration gradient, c, y component	mol/m^4	cy
dflux_c_y_chcd	Diffusive flux, c, y component	mol/(m^2*s)	-Dyx_c_chcd * cx-Dyy_c_chcd * cy
cflux_c_y_chcd	Convective flux, c, y component	mol/(m^2*s)	c * v_c_chcd
tflux_c_y_chcd	Total flux, c, y component	mol/(m^2*s)	dflux_c_y_chcd+cflux_c_y_chcd
beta_c_x_chcd	Convective field,	m/s	u_c_chcd

	c, x component		
beta_c_y_chcd	Convective field, c, y component	m/s	v_c_chcd
grad_c_chcd	Concentration gradient, c	mol/m^4	sqrt(grad_c_x_chcd^2+grad_c_y_chcd^2)
dflux_c_chcd	Diffusive flux, c	mol/(m^2*s)	sqrt(dflux_c_x_chcd^2+dflux_c_y_chcd^2)
cflux_c_chcd	Convective flux, c	mol/(m^2*s)	sqrt(cflux_c_x_chcd^2+cflux_c_y_chcd^2)
tflux_c_chcd	Total flux, c	mol/(m^2*s)	sqrt(tflux_c_x_chcd^2+tflux_c_y_chcd^2)
cellPe_c_chcd	Cell Peclet number, c	1	h * sqrt(beta_c_x_chcd^2+beta_c_y_chcd^2)/Dm_c_chcd
Dm_c_chcd	Mean diffusion coefficient, c	m^2/s	(Dxx_c_chcd * u_c_chcd^2+Dxy_c_chcd * u_c_chcd * v_c_chcd+Dyx_c_chcd * v_c_chcd * u_c_chcd+Dyy_c_chcd * v_c_chcd^2)/(u_c_chcd^2+v_c_chcd^2+eps)
res_c_chcd	Equation residual for c	mol/(m^3*s)	-Dxx_c_chcd * cxx-Dxy_c_chcd * cxy+cx * u_c_chcd-Dyx_c_chcd * cyx-Dyy_c_chcd * cyy+cy * v_c_chcd-R_c_chcd
res_sc_c_chcd	Shock capturing residual for c	mol/(m^3*s)	cx * u_c_chcd+cy * v_c_chcd-R_c_chcd
da_c_chcd	Total time scale factor, c	1	Dts_c_chcd
U_ns	Velocity field	m/s	
V_ns	Vorticity	1/s	
divU_ns	Divergence of velocity field	1/s	
cellRe_ns	Cell Reynolds number	1	
res_u_ns	Equation residual for u	N/m^3	
res_v_ns	Equation residual for v	N/m^3	
beta_x_ns	Convective field, x component	kg/(m^2*s)	
beta_y_ns	Convective field, y component	kg/(m^2*s)	
Dm_ns	Mean diffusion coefficient	Pa*s	
da_ns	Total time scale factor	kg/m^3	
taum_ns	GLS time-scale	m^3*s/kg	
tauc_ns	GLS time-scale	m^2/s	
res_p_ns	Equation residual for p	kg/(m^3*s)	